1991

Deformation mechanisms and finite strain within the Foreland Imbricate Fan, Sawtooth Range, Montana

James E. Holl
Lehigh University

Deformation Mechanisms and Finite Strain Within the Foreland Imbricate Fan, Sawtooth Range, Montana

by
James E. Holl

A Thesis
Presented to the Graduate Committee
of Lehigh University
in Candidacy for the Degree of
Master of Science
in
Geological Sciences

Lehigh University
1991

This thesis is accepted and approved in partial fulfillment of the requirements for the degree of Master of Science.

12/14/90
(date)

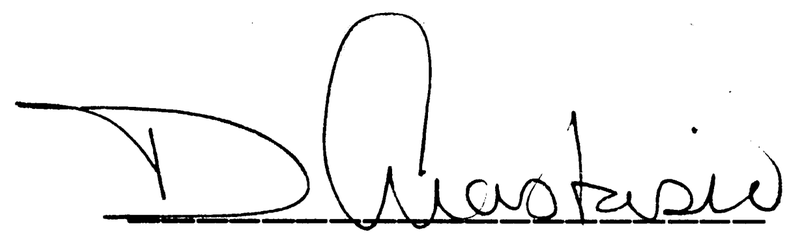

Professor in Charge

Chairman of Department

Acknowledgements

Many people aided in the completion of this thesis. Specifically I would like to thank Dr. David Anastasio for his guidance and advice in all aspects of research and revision of the final paper; Dr. P.B. Meyers and Dr. G. Stephens for their helpful comments and criticisms. I would also like to thank Geosource Inc. for supplying the seismic data, the Montana Bureau of Mines for supplying the subsurface data, and Beth Ihle of the U.S. Forest Service for logistic support.

Financial support for this research was furnished through grants from the American Association of Petroleum Geologists, Sigma Xi, and Standard Oil of California.

Table of Contents

LIST OF TABLES

LIST OF FIGURES

Abstract

Finite strain, deformation mechanisms, and kinematic indicators associated with imbricate fan development have been determined on a variety of scales within several foreland thrust sheets of the central Sawtooth Range, Montana.

A balanced cross section of the central Sawtooth Range, constrained by well, seismic, and surface data indicates a minimum of 60% horizontal shortening (10 km), accommodated by a forward developing imbricate fan which was later truncated by out of sequence movement along the Lewis Thrust. Seismic records delineate a 3.5^{o} westward dipping Precambrian basement and westward thickening of the Precambrian Belt Supergroup. Major detachments within the central Sawtooth Range occur at the base of the Cambrian Steamboat Limestone, at the base of the Devonian Jefferson Formation, and within the Mississippian Allen Mountain Limestone, and the Cretaceous Colorado Group.

Along the base of each thrust sheet, deformation has been partitioned into mesoscopic fault arrays which define brittle deformation zones (BDZs). BDZ width depends on fault displacement but not fault trajectories or subsequent foreland imbrication. The ratio of BDZ width to displacement (1:33) was constant with BDZ widths from 65 - 200 m for faults whose displacements range from 2.5 - 7 km. BDZ bases are characterized by an interlocking network of fault arrays which exhibit great diversity and accommodate

cataclastic flow. BDZ bases are dominated by oblique-slip faults while faults in middle and upper BDZ positions are dominantly dip- or strike-slip. Within the brittle deformation zones, zones of contractional, extensional, or more commonly transport-parallel strike-slip faults dominate and are separated by bedding plane detachments. Tear fault displacements reflect along-strike positions. Fault length/m^2 of outcrop decreases to zero from a maximum of 4 m/m^2 across the BDZs.

On a grain scale, deformation has been accommodated by mechanical twinning, cataclasis, and pressure solution. Finite strain determinations using object and bulk strain techniques delineate a strain ellipsoid with X/Z parallel to the transport direction. Recorded finite strains are relatively small and constant across the thrust sheets and independent of thrust displacement or elevation above the thrust. This observation suggests that these strains reflect post-BDZ deformation, and may be related to the emplacement of the Lewis thrust sheet.

Introduction

Deformation within orogenic belts occurs on a variety of scales through a variety of deformation mechanisms which are each sensitive to environmental conditions such as temperature, total pressure, or fluid pressures (Knipe, 1989). In the foreland regions of a mountain belt deformation generally occurs under sub-greenschist conditions. Under foreland conditions, strains can be accommodated on a megascopic scale by the translation of sheets of rock upwards and towards the foreland along listric or stair-stepped fault surfaces with concomitant folding (Rich, 1934). On a mesoscopic scale, rocks within foreland areas of mountain belts typically deform by discontinuous mechanisms such as fracturing and faulting (Wojtal, 1986). On a microscale common deformation mechanisms include mechanical twinning (Klassen-Neklyudova, 1964), cataclasis (Jaeger, 1959), and pressure solution (Sorby, 1863).

While both grain scale and mesoscale mechanisms are operative within foreland thrust sheets, deformation is commonly dominated by mesoscale mechanisms which may be partitioned into mesoscale fault arrays defining brittle deformation zones (Wojtal, 1986). Some progress has been made towards creating an understanding of the manner in which discontinuous deformation is partitioned within foreland thrust sheets. Price (1967) was able to determine

the relative movement directions within two converging structural salients and to characterize the kinematics of a transverse fault by using minor fault fabrics within Front Range thrust sheets of the Southern Canadian Rocky Mountains . Bielenstein (1969), in a study of the same region of the Canadian Rockies, used plan view variations in minor faults to characterize strike-parallel extension during thrust sheet emplacement. Wojtal (1986) analyzed the minor fault populations within three Appalachian thrust sheet in order to describe the kinematics of thrust sheet emplacement. In addition to use as kinematic indicators it is possible to use minor fault arrays to determine the orientation and magnitudes of the finite strain if fault displacements and attitudes are known (Wojtal, 1986). If only the fault orientation and the sense and direction of slip is known it is possible to estimate the orientation of the principal strain axes (Arthaud, 1969). If assumptions are made about the relationship between stress directions and fault orientation (Anderson, 1951; Reches, 1978) it is also possible to determine the orientation of the stress axes (Angelier, 1979; Etchcopar et al., 1981; Aleksandrowski, 1985; Reches, 1987) and it may be possible to determine the relative magnitudes of the stress axis (Angelier, 1984 and 1989).

Carbonate deposits are common constituents of thrust belts. One component of fully understanding the processes by which thrust belts deform is understanding the mechanisms by which carbonate thrust sheets deform. The goal of this study is to characterize, on a

variety of scales, the manner in which foreland carbonate thrust sheets deform during mountain building.

In order to create a more complete understanding of BDZ development within foreland carbonate thrust sheets, four well exposed thrust sheets within the Sawtooth Range, Montana (Figure 1) were studied. The Diversion, French, Norwegian. and Beaver thrust sheets were selected because of the availability of fresh road cuts and similar hanging-wall and foot-wall lithologies. Selection of these four thrust sheets allowed displacement, and position within the thrust sheet to be isolated as variables in order to study BDZ development. In the hanging-walls of each thrust sheet mesoscale structural data and samples, for grain scale analysis, were collected continuously throughout the exposed Mississippian sections. Data collected included approximately 1000 minor fault measurements and 14 finite strain determinations.

After Norris (1958), contraction faults were defined as those which shorten bedding and extension faults were defined as those which extend bedding. For this study, strike-slip faults were defined as those whose movement direction was less than 30° from strike. Using these criteria eight classes of minor faults are possible (Figure 2): 1) those accomplishing range parallel contraction; 2) those accomplishing range perpendicular contraction (synthetic and antithetic contraction faults); 3) those accomplishing range-parallel extension; 4) those accomplishing range-perpendicular extension (antithetic and synthetic extension);

and 5) strike-slip faults, including both transport-parallel and range-parallel types. These fault types were all found within the imbricates of the central Sawtooth Range.

The results of the meso- and grain-scale analyses were then compared with fault shapes, fault displacements, and position within the thrust belt in order to determine the significant variables affecting the intensity and style of thrust sheet deformation. These analyses provide important insight into the kinematics of thrust sheet emplacement, the manner in which BDZs develop within these thrust sheets, and the way strain is partitioned within the BDZ.

Geologic Setting

Structural Setting

The Montana Disturbed Belt (Figure 1) is a segment of the North American Cordillera which extends from Alaska to Mexico (Mudge, 1970). The Montana Disturbed Belt is characterized by three subbelts (Figure 1); an internal zone containing imbricated Precambrian rocks, a central zone containing Paleozoic imbricates, and an external zone containing exposures of imbricated synorogenic Mesozoic rocks. The Sawtooth Range is coincident with subbelt II and is an arcuate zone of north-south trending, closely

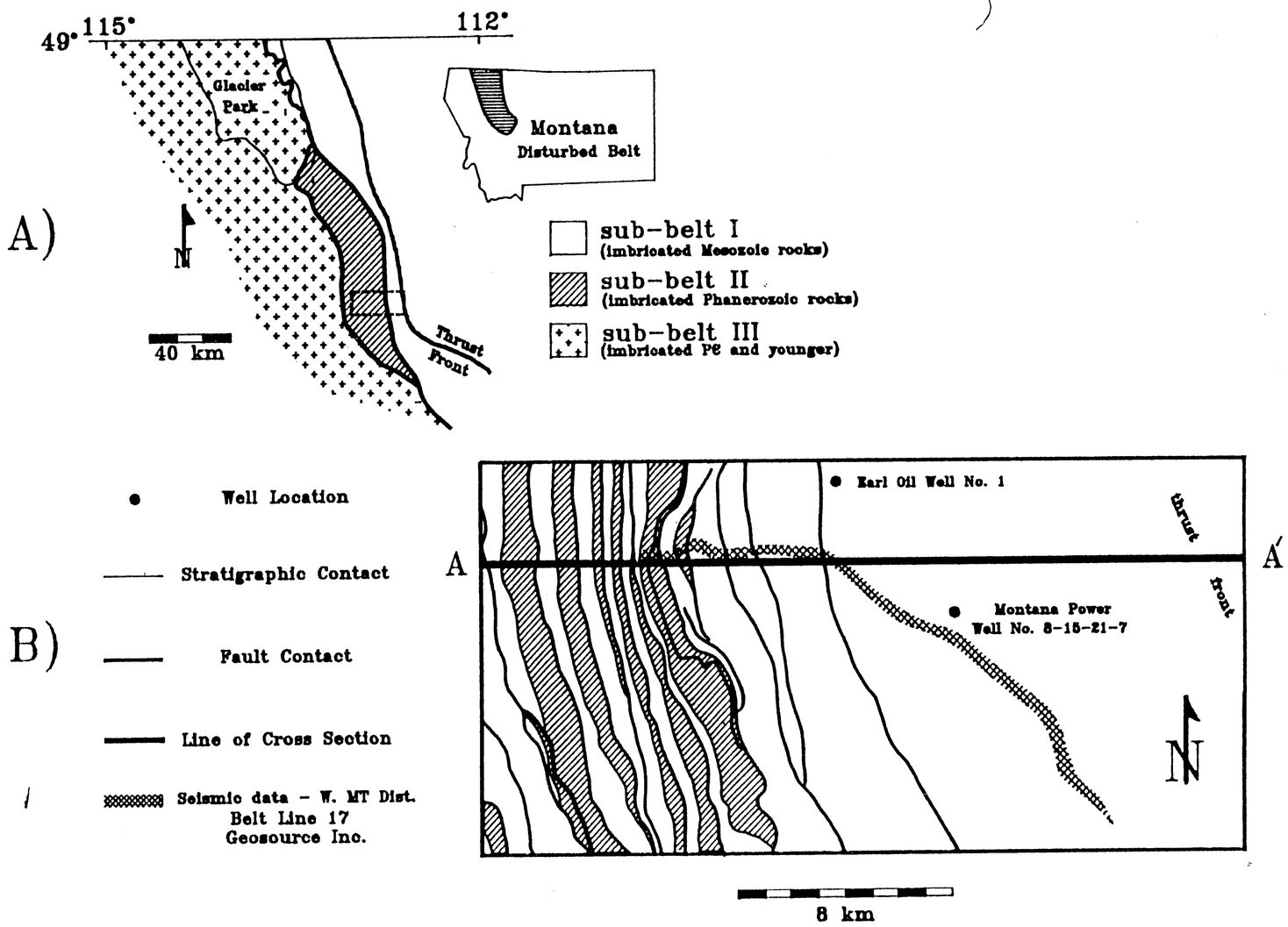

Figure 1 - A) Generalized geologic map of northwestern Montana B) Generalized geologic map of the central Sawtooth Range (after Mudge, 1982) (cross section A- A' shown in figure 4).

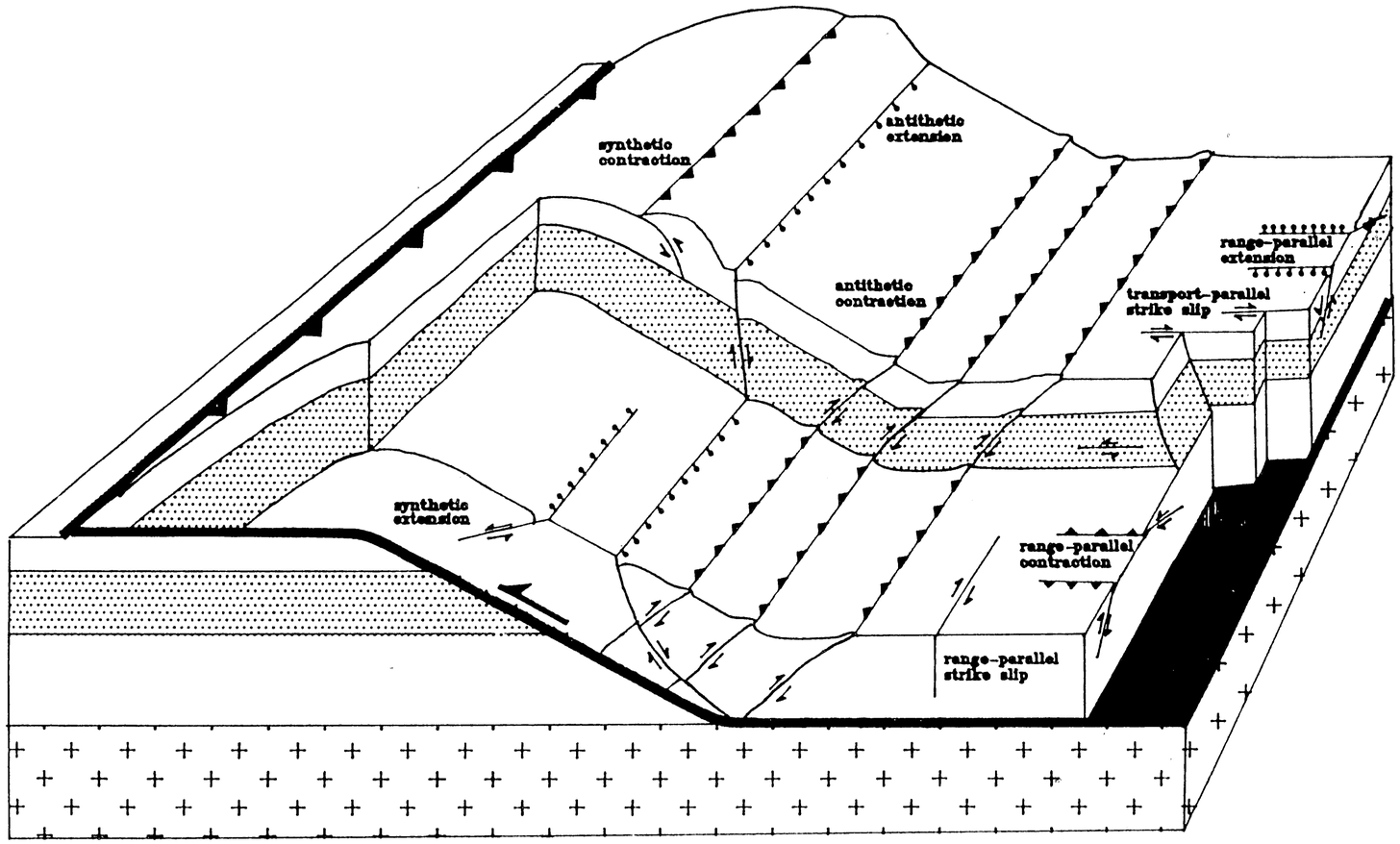

Figure 2 - Schematic thrust sheet defining the minor fault types used in this study.

spaced, westerly dipping imbricate thrust sheets and associated folds which formed during the Late Cretaceous to early Paleocene (Mudge, 1982).

Stratigraphy

The Sawtooth Range exposes Precambrian through Cretaceous strata (Figure 3). The Precambrian Belt Supergroup consists primarily of marine clastics with some carbonate units (Mudge, 1982). The thickness of the Precambrian rocks ranges from 400 m to 600 m (determined from seismic reflection data) in the eastern part of the Sawtooths but increases rapidly to the west where it exceeds 10,000 m (Mudge, 1982).

The Cambrian stratigraphic sequence consists predominantly of carbonates with a few relatively thin clastic units. The thickness of the Cambrian succession ranges from 300 to 1000 m (Mudge, 1982).

The Devonian section consists of the Maywood, Jefferson, and Three Forks Formations. The Devonian units are dominantly dolomites and limestones although siliciclastic mudstones and evaporite-solution breccias occur (Mudge, 1982).

Overlying the Devonian units are Mississippian carbonates, of the Allan Mountain Limestone and Castle Reef Dolomite. These units are characterized by interbedded marine limestones and dolomites, with the percentage of dolomite increasing up-section (Mudge,

Formation	Thickness	Age
Montana Group	825 - 1900 m	Upper Cretaceous
Colorado Group	415 - 900 m	Lower Cretaceous
Ellis Group	55 - 285 m	Jurassic
Castle Reef Dolomite	70 - 265 m	Mississippian
Allan Mountain Limestone	130 - 220 m	
Three Forks Fm	15 - 170 m	Devonian
Jefferson Fm	125 - 265 m	
Maywood Fm	20 - 110 m	
Devils Glen Dolomite	30 - 160 m	Cambrian
Switchback Shales	20 - 75 m	
Steamboat Limestone	55 - 100 m	
Pentagon Sh.	0 - 85 m	
Pagoda Ls.	25 - 115 m	
Dearborn Ls.	65 -140 m	
Damnation Ls.	30 - 65 m	
Gordon Shale	40 - 85 m	
Flathead Ss	13 - 39 m	
Belt Supergroup	0 - 9660 m	Proterozoic Y

Precambrian crystalline basement

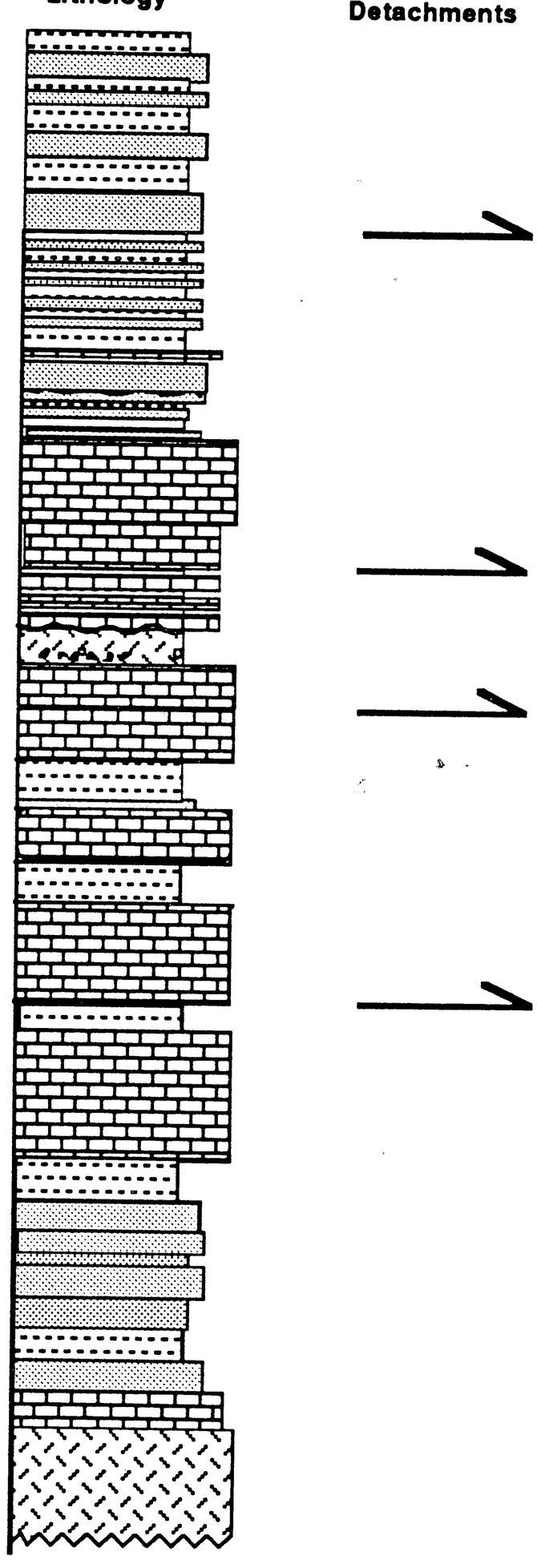

Lithology

Sawtooth Detachments

Figure 3 - Stratigraphic column of western Montana (after Mudge, 1982). The primary horizons of Sawtooth detachments are indicated.

1982). These carbonates are commonly coarse grained and contain crinoid stems or columnals, occasionally in enough abundance to classify the rocks as encrinites.

A succession of Jurassic and Cretaceous marine and non-marine foreland basin clastic sediments which are in part synorogenic unconformably overlies the Mississippian carbonates (Mudge, 1982).

Regional Scale Deformation

In order to constrain thrust belt geometry, the amount of regional scale shortening, and individual thrust sheet displacement a balanced cross section was constructed through Subbelts 1 and 2 of the Montana Disturbed Belt (Figure 1). The eastern edge of the cross section was pinned in undeformed rocks of the foreland.

Subbelt 2 of the central Sawtooth Range contains the Devonian through Cretaceous section of the stratigraphy. Deformation within the Devonian and Mississippian units of Subbelt 2 is characterized by widely spaced imbricate thrust faults and associated folding (Figure 4). Major detachment surfaces within the Mississippian and Devonian rocks occur at the base of the Devonian Jefferson Formation and in the Mississippian Allan Mountain Limestone. Subbelt 1 contains rocks of Jurassic and Cretaceous age. The style of deformation within the Jurassic and Cretaceous rocks of Subbelts 1 and 2 is characterized by abundant imbricate thrust

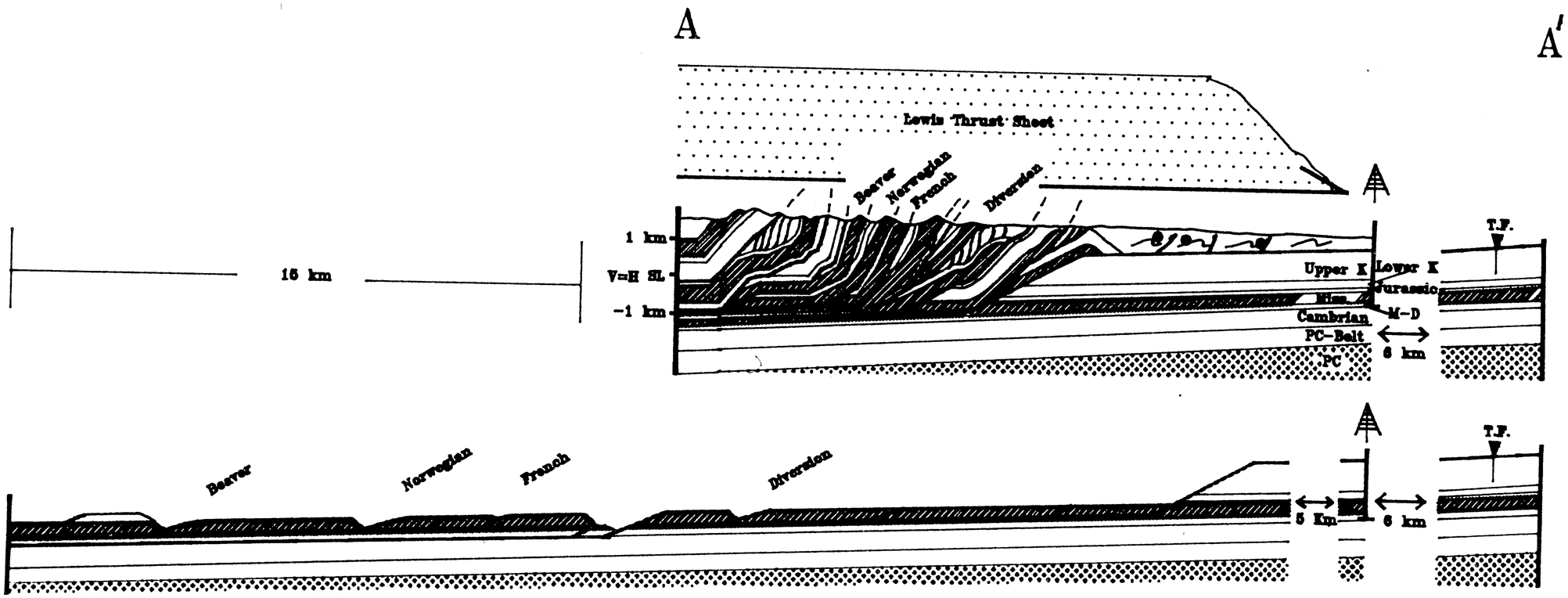

Figure 4 - Restored and deformed cross sections along A - A' through the central Sawtooth Range (see figure 1 for line of section). Dots represent sampling localities for paleotemperature estimates (Clayton et al., 1982). The hypothesized position of the Lewis thrust sheet is also represented.

faults with relatively small offsets (Mudge, 1982) and tight asymmetric folds, with major detachment surfaces occurring in the Cretaceous Colorado Group. The thrust sheets of the central Sawtooth Range become progressively steeper towards the hinterland suggesting that the imbricates formed in foreland progression (Jones, 1971). The restored section (Figure 4) indicates that spacing between the imbricates is inconsistent.

The deformed Paleozoic rocks of the Sawtooth Range overlie unimbricated Precambrian rocks. The thickness of the allochthonous Belt Supergroup was determined using seismic reflection and well data. Thicknesses ranged from approximately 400 m at the thrust front to greater than 600 m at the western edge of Subbelt 2. This thickness estimate is in contrast to estimates of approximately 1500 m for Belt thickness at the eastern edge of the belt by Mudge and Earhart (1983). The dip of the underlying Precambrian crystalline basement was 3.5° to the west and was determined using several seismic profiles located in west-central Montana. This estimate of basement dip is in good agreement with estimates of 3-4° in the Canadian Rockies (Bally et al., 1966) and 2-3° determined from regional structure contour maps on the top of Precambrian crystalline rocks (Mudge, 1982).

Total horizontal shortening across this portion of the belt is approximately 60% (10 kilometers). This estimate of shortening is substantially lower than the approximately 100% of shortening

faults with relatively small offsets (Mudge, 1982) and tight asymmetric folds, with major detachment surfaces occurring in the Cretaceous Colorado Group. The thrust sheets of the central Sawtooth Range become progressively steeper towards the hinterland suggesting that the imbricates formed in foreland progression (Jones, 1971). The restored section (Figure 4) indicates that spacing between the imbricates is inconsistent.

The deformed Paleozoic rocks of the Sawtooth Range overlie unimbricated Precambrian rocks. The thickness of the allochthonous Belt Supergroup was determined using seismic reflection and well data. Thicknesses ranged from approximately 400 m at the thrust front to greater than 600 m at the western edge of Subbelt 2. This thickness estimate is in contrast to estimates of approximately 1500 m for Belt thickness at the eastern edge of the belt by Mudge and Earhart (1983). The dip of the underlying Precambrian crystalline basement was 3.5° to the west and was determined using several seismic profiles located in west-central Montana. This estimate of basement dip is in good agreement with estimates of 3-4° in the Canadian Rockies (Bally et al., 1966) and 2-3° determined from regional structure contour maps on the top of Precambrian crystalline rocks (Mudge, 1982).

Total horizontal shortening across this portion of the belt is approximately 60% (10 kilometers). This estimate of shortening is substantially lower than the approximately 100% of shortening

calculated from Mitra's (1986) cross section.

Mesoscale and grain scale deformation was characterized within the frontal imbricates of the central Sawtooth Range. The Diversion, French, Norwegian, and Beaver thrust sheets have simple one ramp fault trajectories (Figure 4). Stratigraphic separation diagrams as well as field and map evidence indicate that the detachments for these four thrust sheets occur in the Mississippian Allan Mountain Limestone and in the Cretaceous Colorado Group, with the primary ramp occurring in the interval between these two horizons. This fault trajectory is in contrast to a cross section drawn along a similar profile by Mitra (1986) in which a Devonian flat is extended from the Teton River Valley south into the Sun River section. Stratigraphic separation diagrams suggest that the detachment cuts laterally upsection into the Mississippian carbonates north of the Sun River near the north fork of Willow Creek.

Based on organic geochemical analyses in the Cretaceous shales of Subbelts 1 and 2, Clayton and others (1982) estimate that these rocks reached a maximum temperature of approximately 276° C. K/Ar dating indicates that this low grade metamorphic event was concomitant with thrusting in the Sawtooth Range (Hoffman et al.,1976).

Mesoscale Deformation

In the lower portion of each thrust sheet of the central Sawtooth Range, deformation is partitioned into collections of

mesoscopic faults which define brittle deformation zones (BDZs) (Figure 5). Individual minor faults found within any of the thrust sheets are indistinguishable, but the character of the fault collections including spacing between faults, fault attitudes, slip direction, and general patterns of their offsets, change with position in the thrust sheet. At comparable positions within the Diversion, French, Norwegian, and Beaver thrust sheets, minor faults record similar kinematics suggesting that arrays (interlocking networks) of minor faults, not individual faults are the essential components of mesoscale deformation.

The BDZs within each of the thrust sheets were defined as the region in each thrust sheet between the regional thrust surface and the last observed minor fault. The total width of each BDZ was found to be directly related to thrust sheet displacement (Figure 6). Mesoscale faults develop only near the regional thrust surfaces during displacement. As fault displacement increases from 2 km, on the Diversion thrust, to 6 km, on the more hindward Beaver thrust, BDZ thickness increases 65 m to 200 m. Using linear regression, a line of best fit for the data was calculated (Figure 6) and indicates that the ratio of BDZ width to thrust sheet displacement (1:33) was constant for all four thrust sheets. Plotting the continuation of this line, its intersection with the y-axis was found to lie very near the origin suggesting that faults with no displacement would not have BDZ's strengthening the argument that BDZ thickness and displacement are directly related.

Figure 5 - Photomosaic and accompanying sketch show the base of the French Thrust sheet. The emplacement of the French Thrust sheet onto Cretaceous shales resulted in the formation of a BDZ in the hangingwall.

BDZ thickness does not correlate with differences in fault shape (ramp/flat ratio) or the amount of subsequent foreland imbrication which carried more hinterland sheets piggyback.

Because of the lack of recognizable bedding offsets and the poor correlation observed between fault length and offset, determining the amount of strain accommodated by the minor faults was not possible. In order to quantify the relative intensities of mesoscale deformation, the total fault length per m^2 area was determined across each thrust sheet (Figure 7). From these data it is apparent that fault intensity is always higher at the base of the BDZ than at the top of the BDZ (Figure 7). However, fault intensities within the BDZ may vary irregularly. In the French and Norwegian thrust sheets the intensity of mesoscale deformation decreases logarithmically from $4m/m^2$ to $0m/m^2$ at the top of the BDZ. However, in the Diversion and the Beaver, the pattern is more complicated; large peaks of localized faulting occur within these thrust sheets. The peaks in the total minor fault intensity are primarily the result of localized zones of transport-parallel strike-slip faulting isolated by bedding plane detachments (Figure 8).

Changes in fault intensity are associated with changes in fault kinematics. In order to characterize the populations of minor faults present within each BDZ, minor fault data were analyzed stereographically as fault poles with slip linears. Slip linears represent a portion of the great circle containing both the fault pole and the slip direction with the relative movement sense of the hangingwall indicated by an arrow (Figure 9; Hoeppener, 1953;

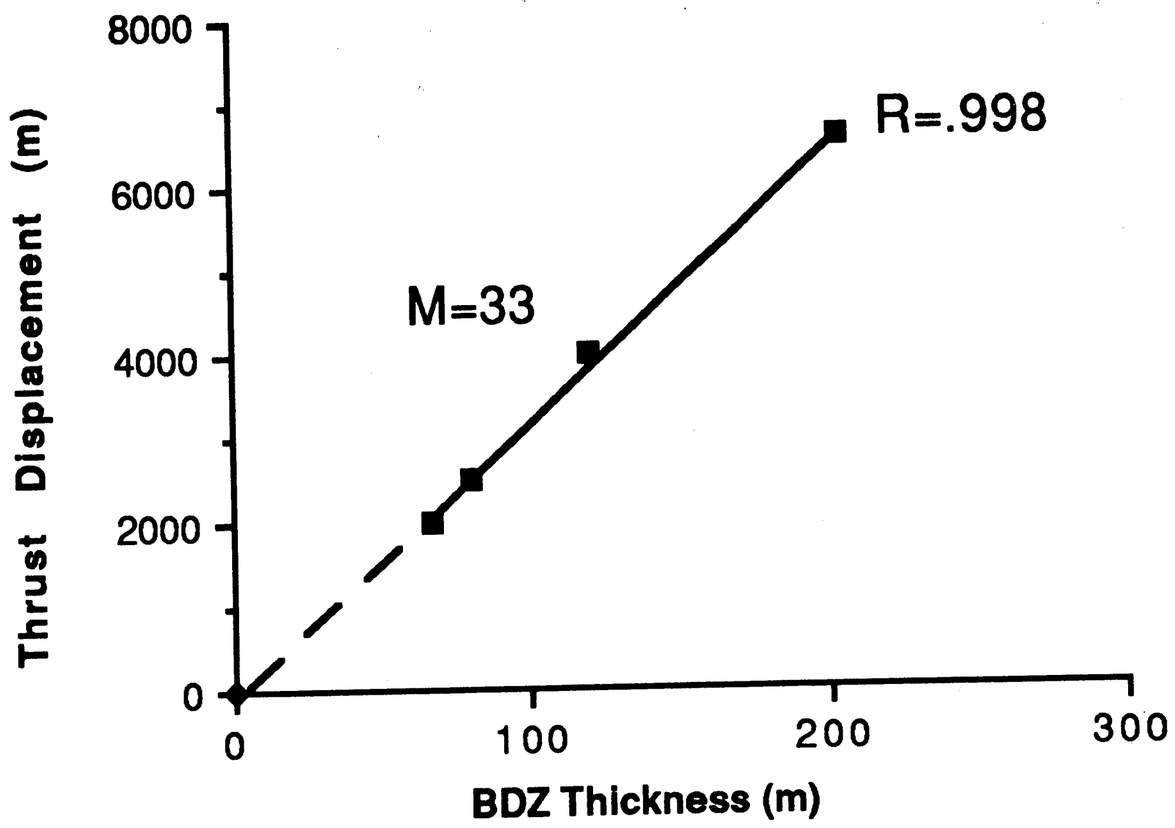

Figure 6 - Graph of BDZ thickness vs. regional thrust displacement.

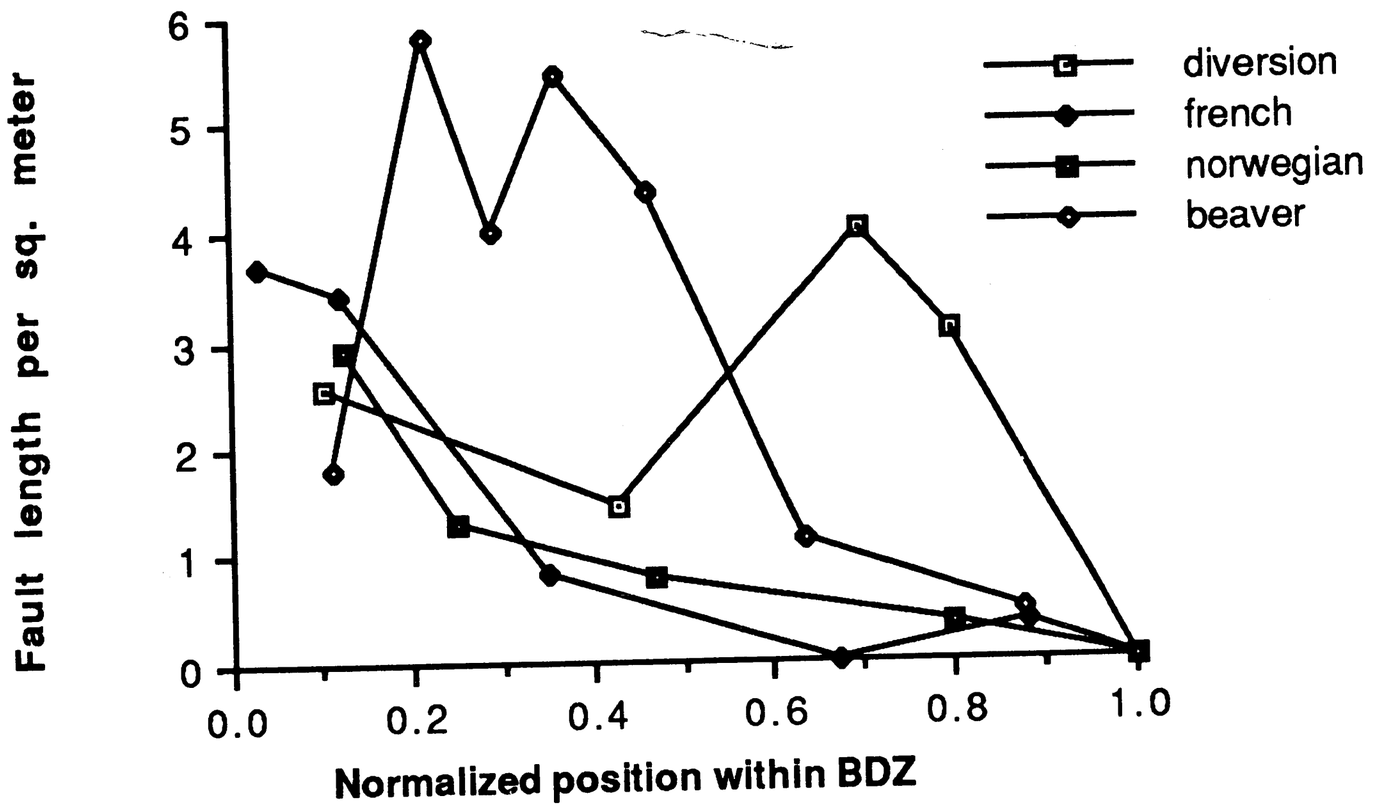

Figure 7 - Plots of total fault length as a function of distance from the base of the thrust sheet for the four Sawtooth thrust sheets.

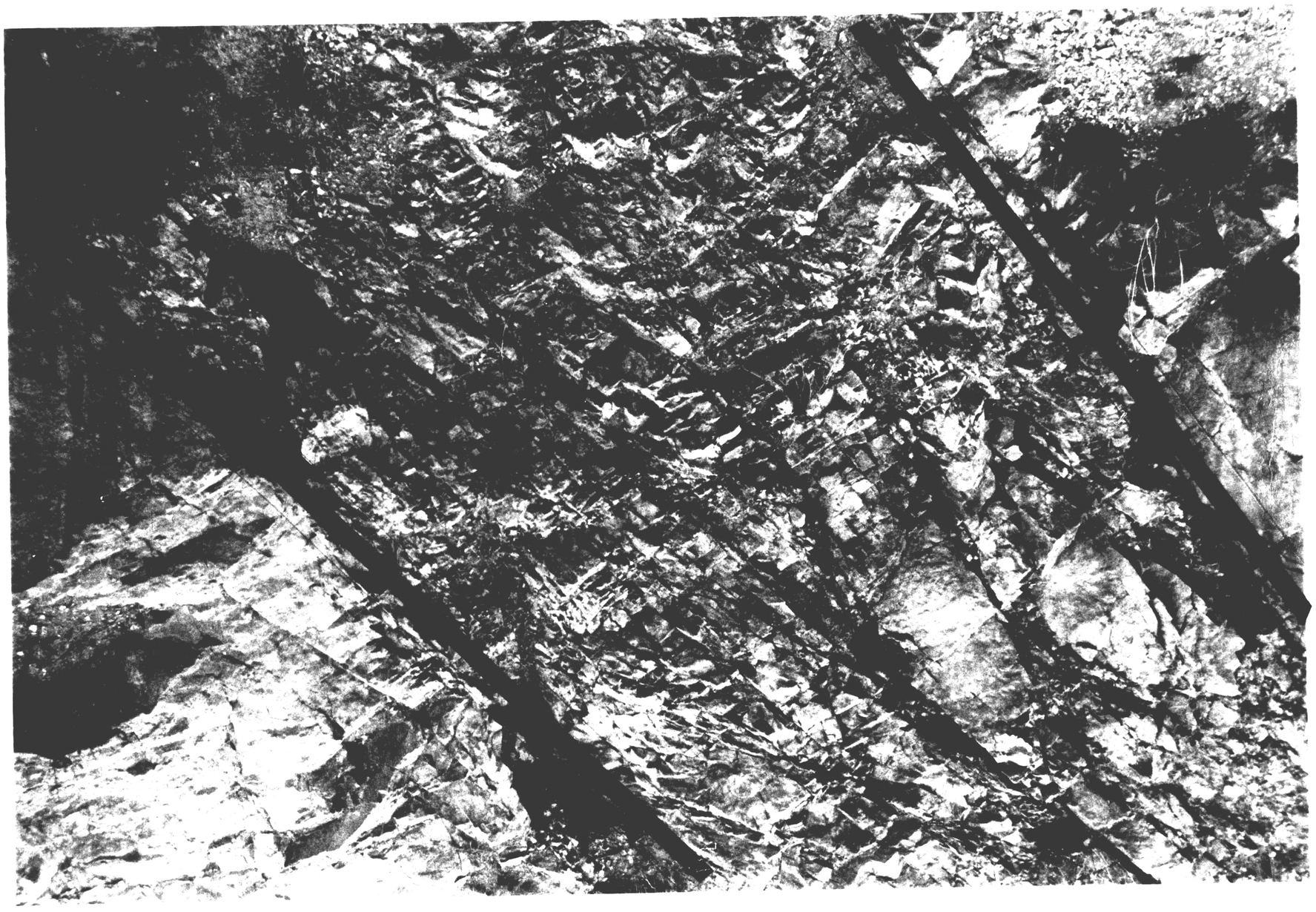

Figure 8 - Example of a shattered zone within the Beaver thrust sheet.

A)

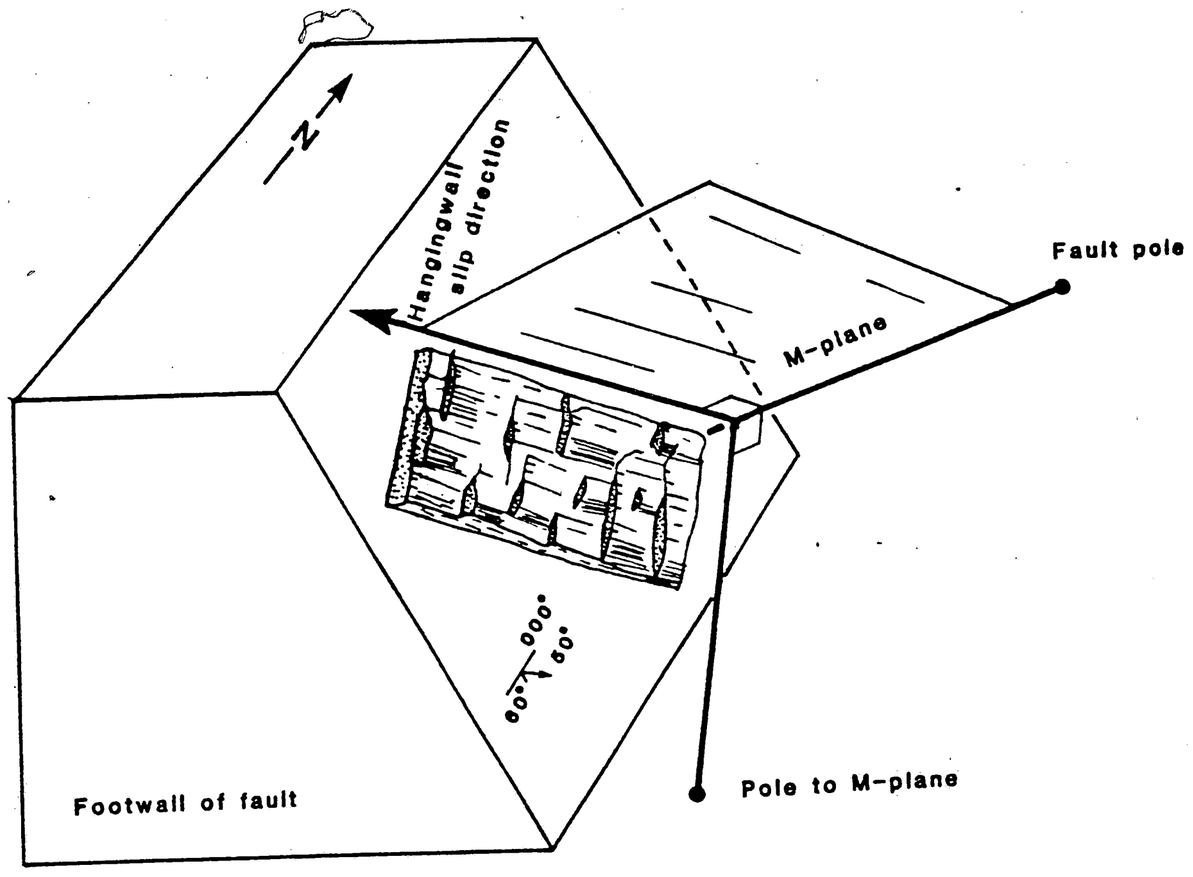

B)

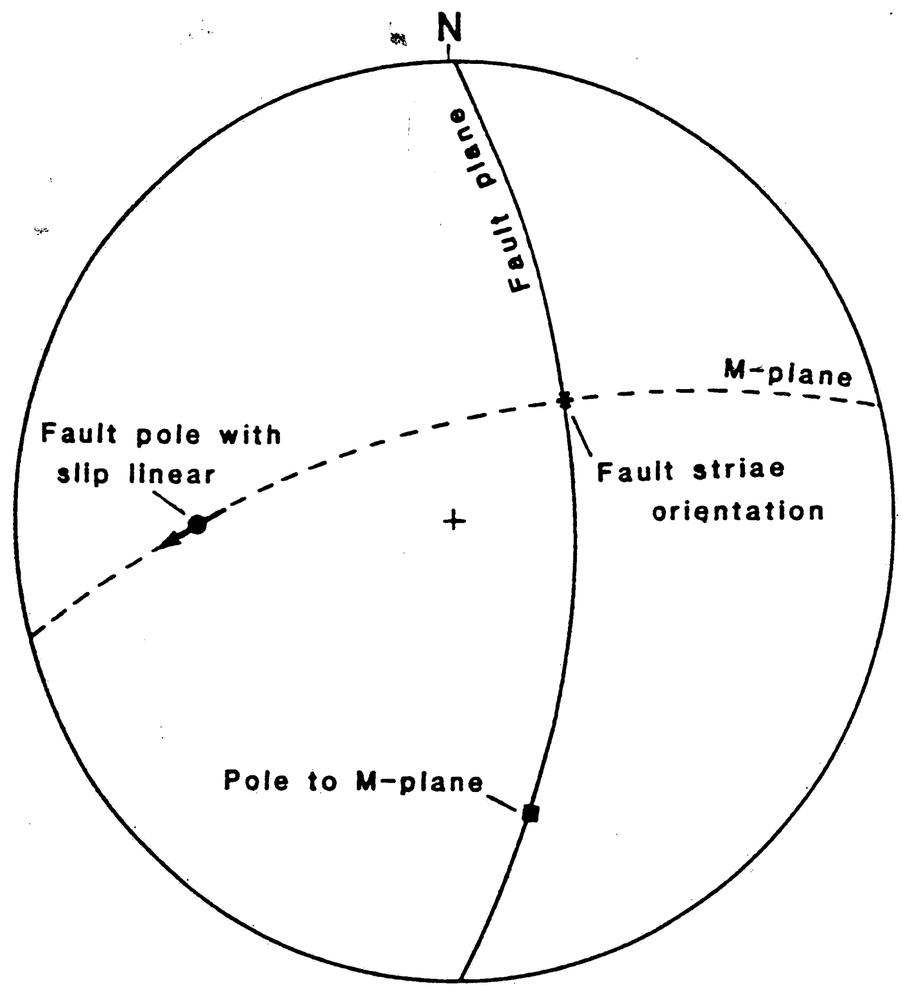

Figure 9 - A) Block diagram showing the commonly analyzed kinematic features on a fault plane. B) An equal area plot of the slip linear and the great circle traces of the fault plane and M-plane. (from Anastasio, 1987).

Anastasio, 1987). This type of plot simplifies the interpretation of minor fault data by allowing the orientation and the kinematics of each fault to represented on one stereonet plot.

Faults of similar attitude and movement sense were averaged using the Bingham axial distribution technique. In order to construct an average slip linear plot both the m-planes and the fault planes were averaged. Averages were considered statistically valid if eigenvalues for both averages exceeded 0.80 and average plots were considered valid if >80% of the faults in a station were accounted for (Figure 10 and Table 1). These cut offs were used to simplify the kinematic picture of deformation within the BDZs without losing the essence of the deformation pattern.

Data recorded continuously across each BDZ naturally divides itself into 3 regions defined by differences in the character of the fault arrays present including fault types, fault diversity, and the intensity of faulting (Figure 11). Region boundaries within the BDZ are gradational. For all thrust sheets the boundary between the lower, most deformed region, and the middle region ranges in position from 18-23% of the total BDZ thickness, while the boundary between the middle and upper, least deformed region, ranges from 60-70%.

Although each thrust sheet is different some generalizations about the kinematics of the BDZs for each sheet can be made. The base of a BDZ has a higher diversity of fault types than the rest of

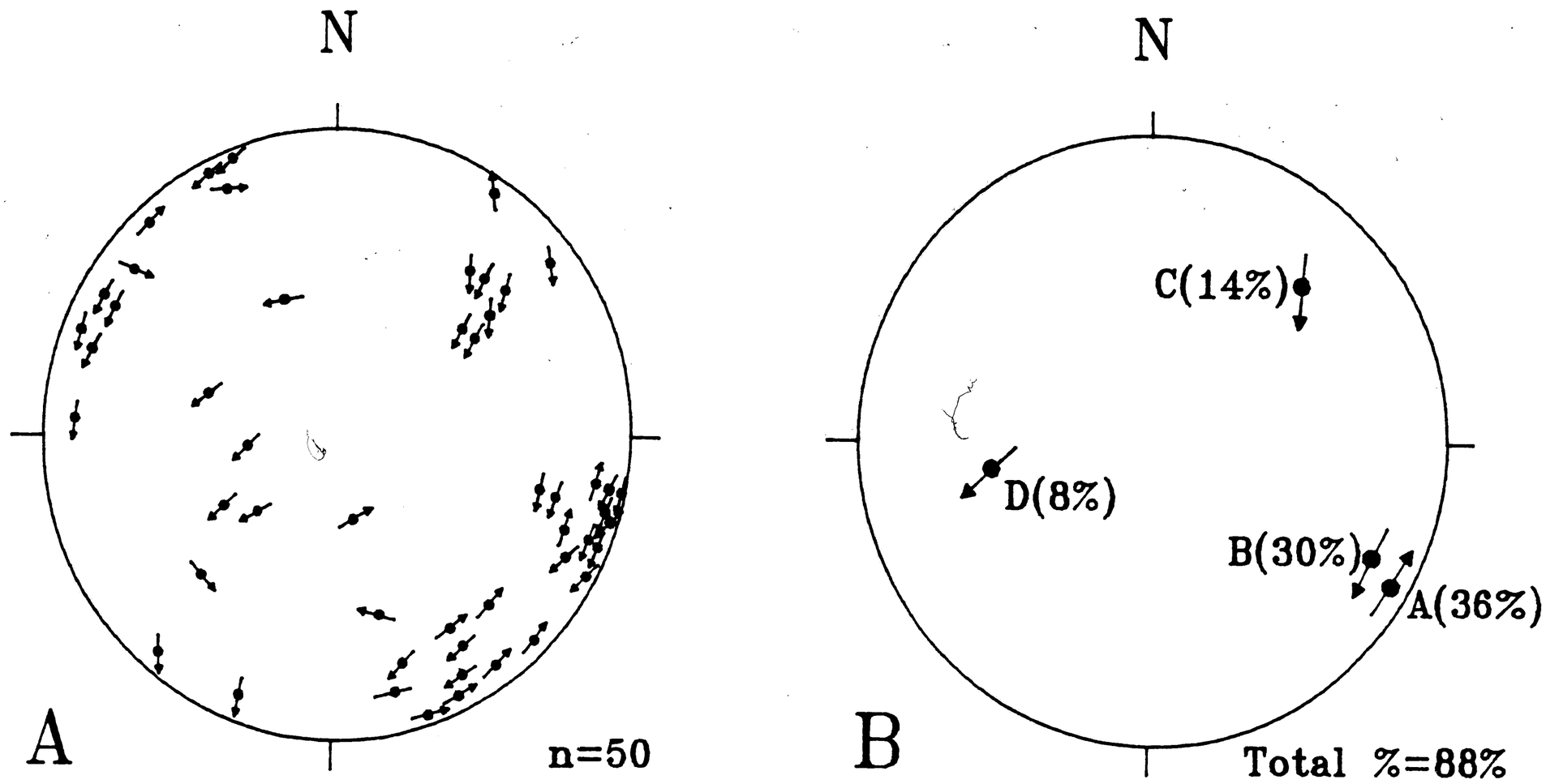

Figure 10 - A) A slip linear plot of minor faults found within a portion of the middle of the Beaver BDZ. B) Reduced data with the percentage of data points projected into each average slip linear indicated.

Population	N	% total	k Faults	k M-planes
A	18	36%	.8300	.8700
B	14	30%	.8400	.8800
C	7	14%	.9800	.9500
D	4	8%	.9200	.8100

Table 1 - Statistical data describing the clustering of data points for the fault populations shown in Figure 10.

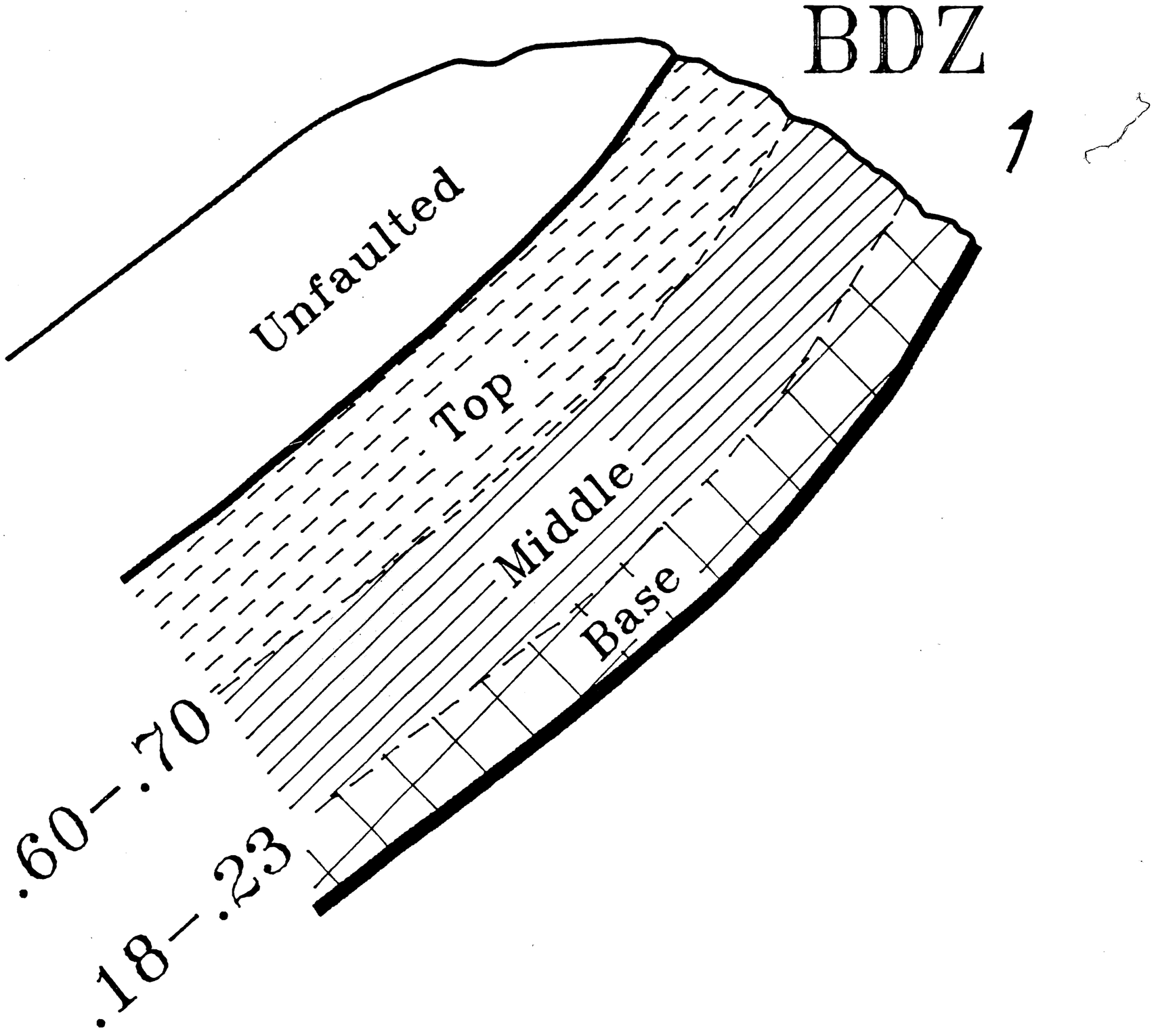

Figure 11 - Schematic representation of a thrust sheet showing BDZ (shaded) subdivision boundaries. Percentages represent the range in position of subdivision boundaries as a function of total BDZ thickness for Sawtooth Range thrust sheets. Hatching patterns are used in following figures to denote subzones within the BDZ.

the BDZ, containing all of the fault types found in the remainder of a given thrust sheet (Figure 12). The minor fault arrays found at the base of the BDZ were dominated by range parallel oblique contraction and strike-slip faults and tear faults. Minor faults with transport-parallel motion were rare in the basal portion.

The middle portion of the BDZ is defined by a significant decrease in fault diversity and particularly in the relative importance of minor faults with range-parallel motion. In general, the most significant classes of minor faults found within the middle portion of the BDZ are tear faults and transport-parallel contraction and extension faults (Figures 12 and 13). These fault types are commonly localized into thin contractional or extensional deformation zones (shattered zones)(Figures 8 and 13). In the middle of the Diversion and Beaver BDZs the most prevalent type of minor faults are tear faults which result in large peaks in total fault intensity (Figure 13). The middle of the Norwegian and French BDZs are not dominated by tear faults, but do contain a substantial percentage of transport-parallel contraction and extension faults.

The top of a BDZ is characterized by a low diversity of minor faults and is dominated by minor faults which move material parallel to the transport direction (Figures 12 and 13). The fault types found within the upper portion of the BDZ are dominantly dip or strike slip including transport parallel contraction and extension faults. In the Diversion and Beaver BDZs tear faults are common.

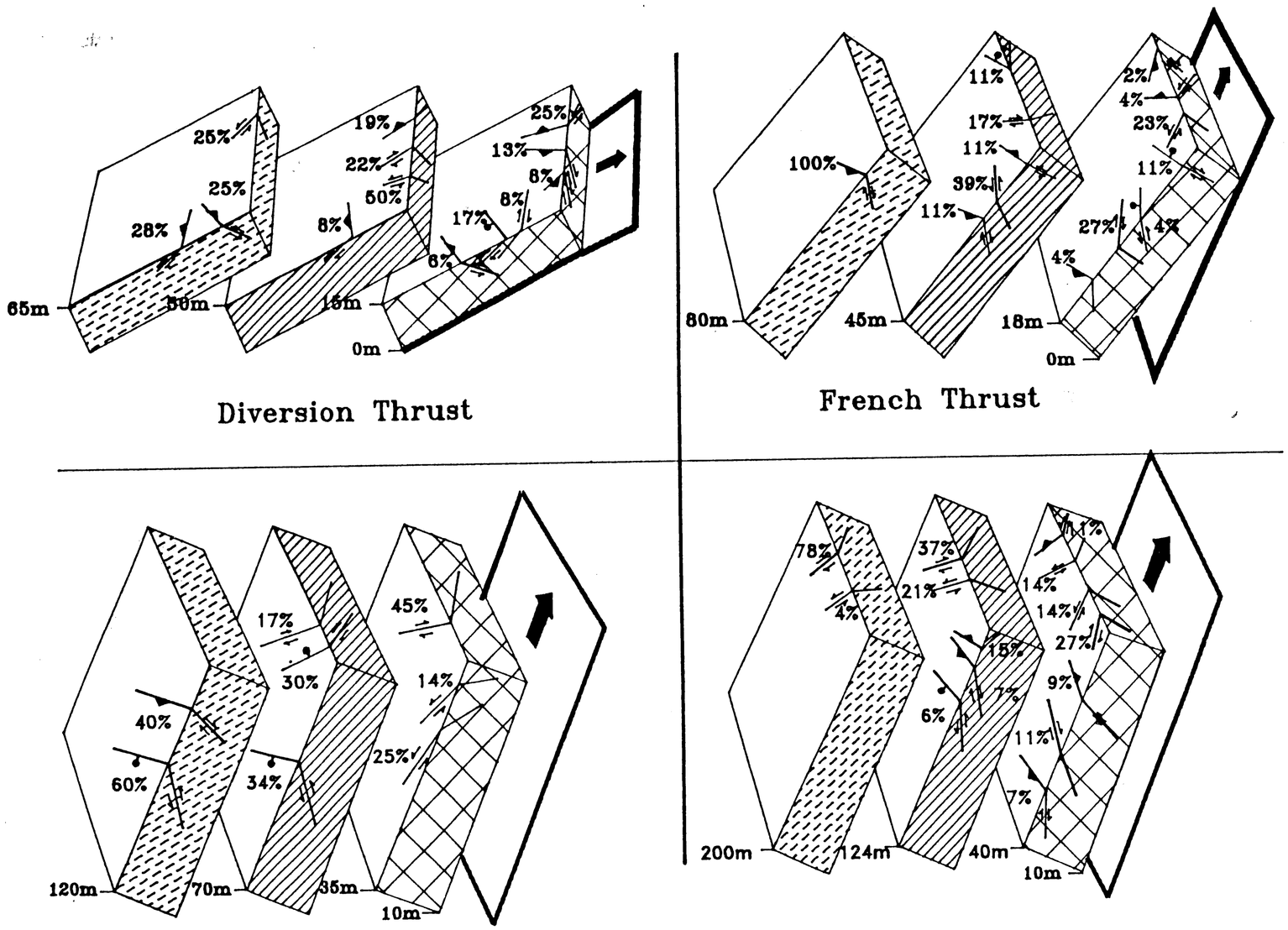

Figure 12 - Block diagrams showing the distribution of fault populations within each of the three BDZ stations for the four thrust sheets studied.

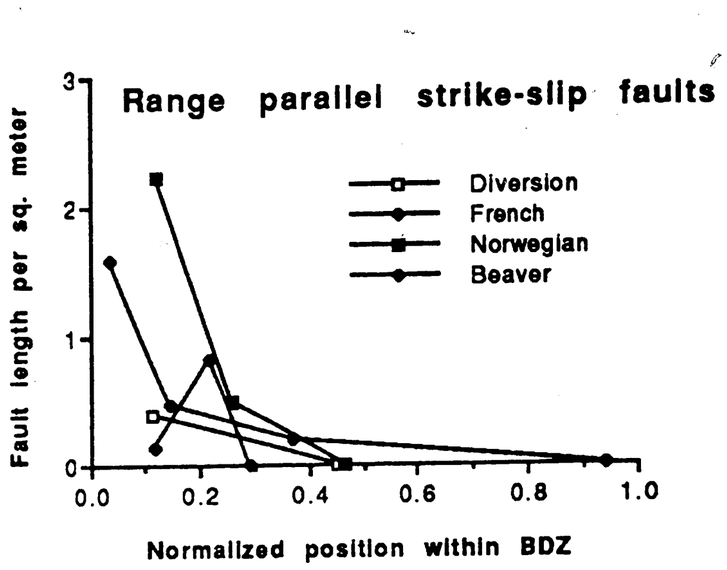

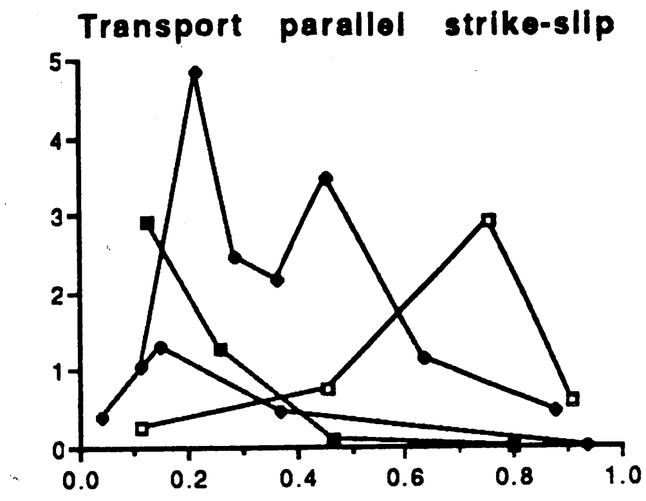

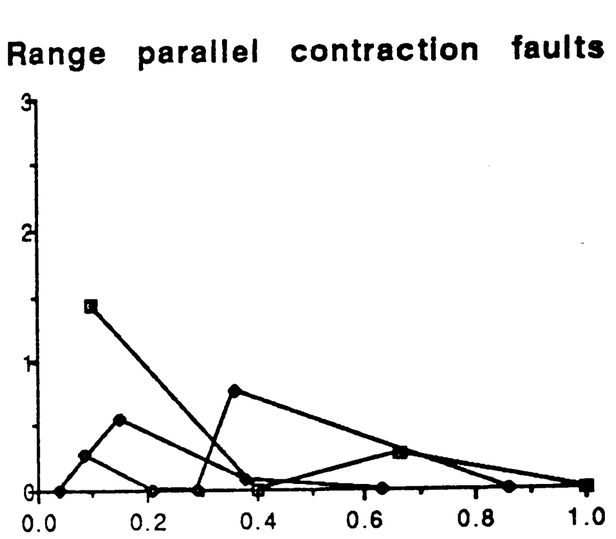

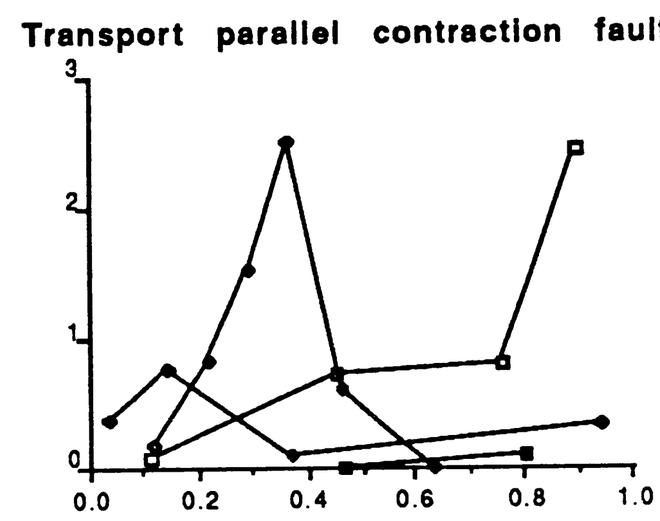

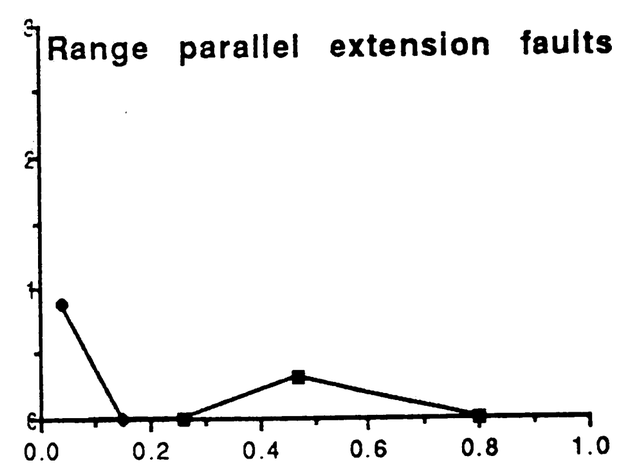

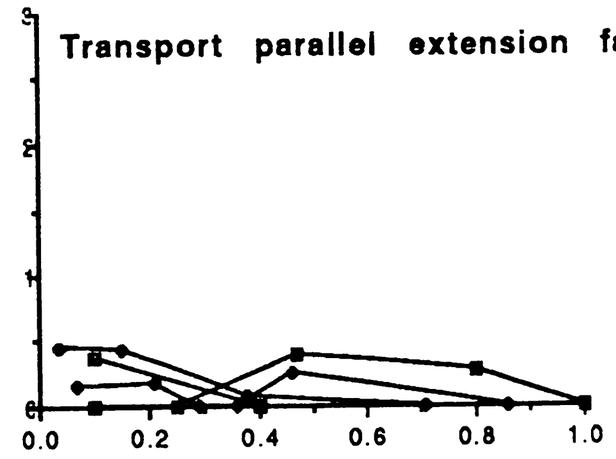

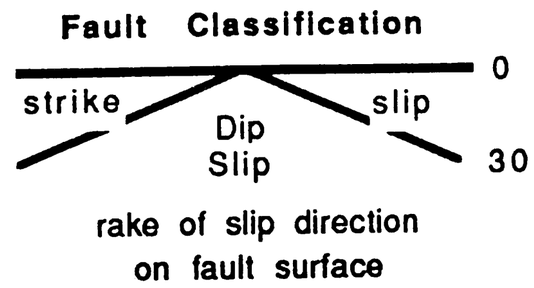

Figure 13 - Graphs showing the variations in the intensity of the individual fault populations as a function of normalized position within the BDZ's of each of the four thrust sheets.

Tear faults are in general the most penetrative class of minor fault found within these BDZs (Figures 12 and 13). Both right and left-lateral faults commonly occur within the same fault arrays, however, one movement sense dominates depending on position within the thrust sheet. In locations north of the middle of a thrust sheet left-lateral faults dominate while in locations toward the southern tip, right-lateral faults dominate.

Grain-scale Deformation

In conjunction with the analysis of regional and mesoscale deformation, grain-scale deformation within the Sawtooth carbonates was also studied. Dominant grain scale deformation mechanisms were determined from microscale observations. The occurrence of tectonic stylolites, sutured grain contacts, and mineral overgrowths indicate that pressure solution was one of the operative mechanisms (Figure 14a). Also, the presence of fractured and fragmented grains indicates cataclasis (Figure 14b) and the presence of mechanical twins (Figure 14a) indicates that low temperature crystal plasticity was important. Finite strain was determined across each thrust sheet (Figure 15). Due to limited exposure adjacent to regional thrusts, only the Diversion and French sheets were sampled within the lowest 5% of the BDZ. Finite

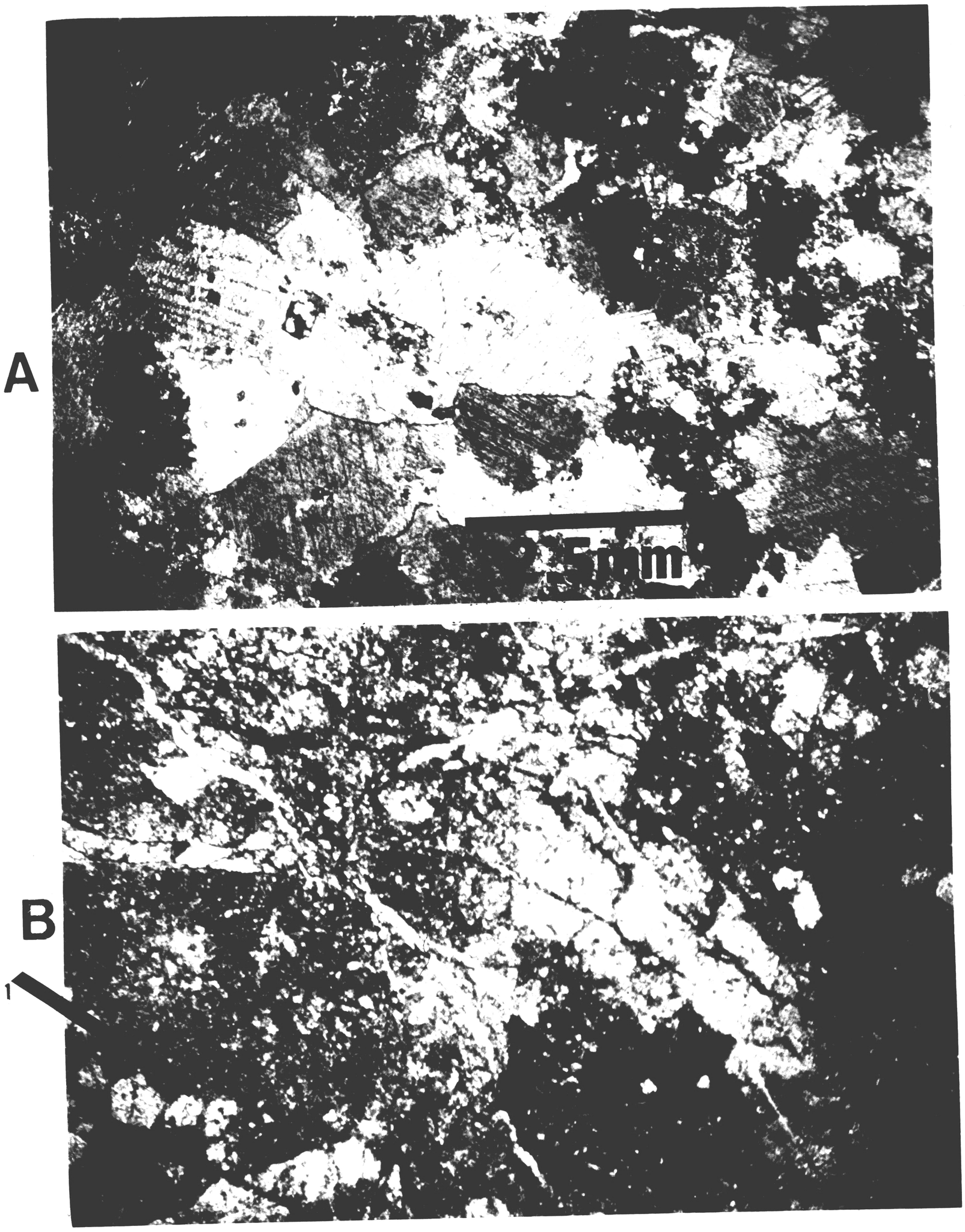

Figure 14 - Photomicrographs of grain-scale deformation features found within the carbonates of the Sawtooth range A) mechanically twinned crinoid columnals displaying sutured grain contacts, and B) fractured grains from a cataclasite layer found at the base of the French thrust sheet, a poorly developed foliation (S1) is also developed.

strain was measure in both the cross-section plane and in a fault-parallel plane, using a variety of object and bulk strain techniques, including the Fry method (Fry, 1979), Normalized Fry [Erslev, 1988; and Erslev and Ge, 1990], and Rf/Phi (Dunet, 1969) (Figure 15). The planes in which finite strain was measured were in general found to be principal planes allowing the three dimensional strain ellipsoid to be determined.

In general, the magnitude and orientation of finite strain within all of the thrust sheets is remarkably constant and very small. Axial ratios in the cross section plane (XZ) ranged from 1.40 to 1.50 while axial ratios (XY) in the fault plane averaged 1.30 and ranged from 1.20 to 1.50 (Figure 15). These finite strain ellipsoids are slightly prolate having average k-values of 2.00. Directly adjacent to the Diversion thrust finite strain is significantly higher, with an axial ratio of 2.20 in the cross-section plane and 1.90 in the fault plane. These data suggest that a narrow (<10m) zone of higher penetrative strain, possibly related to fault propagation or emplacement, develops in the hanging-wall even when displacement is small.

The orientation of the strain ellipsoids was also relatively constant within each thrust sheet (Figure 15). The XY plane of the strain ellipsoid ranges in orientation from subparallel to moderately inclined (<30^{o}) with respect to bedding, whereas the XZ plane is oriented subperpendicular to the strike of

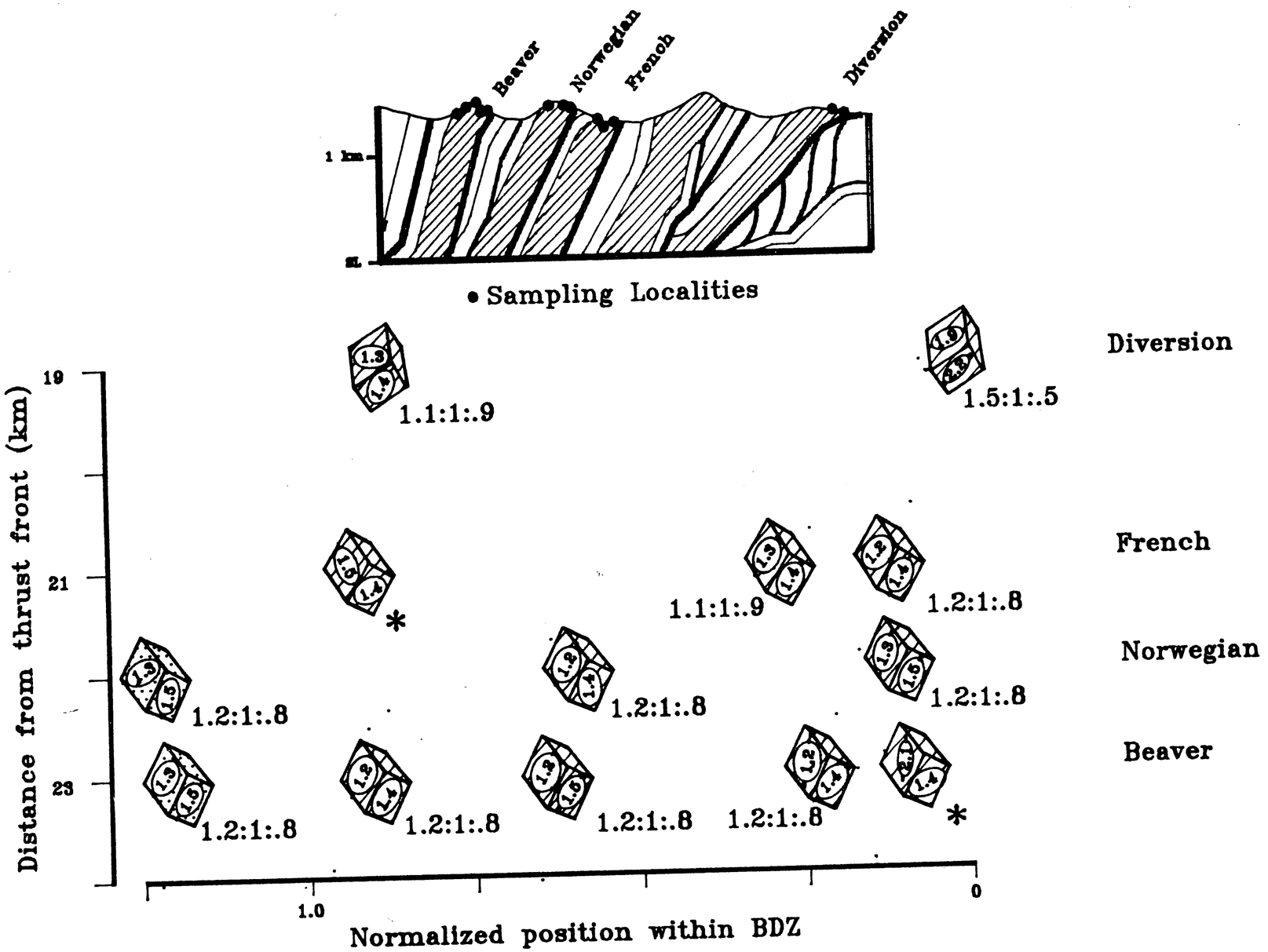

Figure 15 - Three dimensional finite strains determined along the cross section traverse, plotted as function of normalized distance within the BDZ and distance from the thrust front. Sample locations are shown in inset (* indicates samples in which principal planes were not measured).

bedding. Strain ellipsoids measured in a fold located in the Teton River Valley have their long axes oriented approximately horizontal independent of bedding orientation.

The development of "protocataclasites" is associated with relatively large finite strains within the lowest 5% of the BDZ. These rocks display a moderate to poorly developed foliation defined by variations in matrix percentage. These bands anastomose and are roughly parallel to the regional thrust. The development of cataclasites at the base of foreland thrust sheets has been recognized previously (Wojtal and Mitra, 1986) and may be important at the base of the Sawtooth Thrust sheets, however the lack of exposure prevents the determination of the extent of cataclasite development.

Discussion

It has been suggested that the Sawtooth Range is a large duplex structure whose roof thrust (the Lewis Thrust) has been eroded leaving the underlying Paleozoic horses exposed (Clayton et al., 1982). Alternatively, the Paleozoic rocks within the Sawtooth Range may represent an imbricate fan developed in the footwall in front of the Lewis thrust sheet. Paleotemperature data acquired within the Sawtooth Range provides important insight into

resolving this problem.

Assuming a geothermal gradient of 2.0°C/100m (Hoffman et al., 1976), 7,800 - 13,800m of overburden would be necessary to produce the observed temperatures. These overburden estimates are not consistent with measured Cretaceous sections or seismic sections which suggest a maximum possible overburden of 1,800 m of Cretaceous strata. The additional 6000-12000 m of overburden necessary to generate paleotemperatures in these rocks is consistent with reported thicknesses of the Lewis Thrust sheet (Clayton et al., 1982), suggesting that the Lewis Thrust sheet did overlie the Sawtooth Range.

Deformation of the Mississippian carbonates within the four frontal thrust sheets of the Sawtooth Range has been partitioned into mesoscale fault arrays which define brittle deformation zones adjacent to the regional thrust fault. The ratio of BDZ width to displacement (1:33) was constant for all four thrust sheets. Similar relationships have been recognized previously. Robertson (1983) found that the ratio of deformation zone thickness to fault displacement for faults found in mines in Montana, Idaho, Colorado, Arizona, and Ontario was 1:100. Hull (1988) used data from a variety of sources including Robertson (1983) and Otsuki (1978) to suggest that there is a general relationship between thickness and displacement (1:63) over 7 orders of magnitude in deformation zone size. However, these correlations are not well defined, the ratio of BDZ thickness to displacement varied by two orders of magnitude,

between 10 and 1000 and are widely scattered on linear plots (Evans, 1990). Possible reasons for this lack of correlation include the use of data from a wide range of rock types and structural conditions (Robertson, 1983 and Evans, 1990). Data from the Sawtooths suggests that there is a good correlation between BDZ thickness and displacement for thrust sheets deforming under the same conditions and containing the same hangingwall and footwall lithologies.

Growth of the BDZ occurs as the lower portion of the thrust sheets strain harden during emplacement. Thrust sheets in the southern Appalachian foreland have behaved in a similar manner (Wojtal, 1986; Wojtal and Mitra, 1986). Wojtal, (1986) suggests that mesoscale deformation develops progressively. Early in the thrust sheet's history an interlocking network of minor faults develops dividing the base of the sheet into a number of blocks (Stearns, 1969). With continued displacement on a regional scale thrust, increasing amounts of displacement are accommodated on the mesoscale faults and intrablock accommodation features, such as fractures and mineral filled veins. These intrablock deformation features may, with continuing thrust sheet displacement, develop into mesoscale faults. Wojtal and Mitra (1986) suggest that the density of minor faults in the lowest portion of the BDZ will eventually reach a limiting value, at which point further deformation is primarily accommodated by the use of existing mesoscopic faults or by widening the BDZ. The uniformity in

relative thicknesses for BDZ stations in the Sawtooth thrust sheets suggests that the BDZs widen uniformly with increased displacement. Rocks which were in a less deformed portion of the BDZ become incorporated in lower portions of the BDZs as the BDZ widens.

In the thrust sheets studied by Wojtal (1986) continued displacement causes intrablock accommodation features to develop ultimately producing a fine grained foliated cataclasite in the blocks immediately adjacent to a regional thrust fault. The reduction in grain size will promote other grain size sensitive deformation mechanisms. At this point the base of the thrust sheet becomes strain softened and further displacement can be accommodated along the regional detachment without significantly increasing the thickness of the BDZ. In the Sawtooths, however, the linearity of the BDZ vs. displacement curve suggests that cataclasites are not yet well enough developed to strain soften the base of the BDZ.

The thrust sheets within the Sawtooth Range have experienced three types of mesoscale strain. First, strains associated with lateral variations in thrust sheet displacement which may be accommodated by transport-parallel strike-slip faults. The type of transport-parallel strike-slip fault which dominates a fault array is dependent on the lateral position of the station within the thrust sheet. This observation is compatible with the bow and arrow model of thrust sheet displacement, which suggests that the

middle portions of a thrust sheet are active for the longest period of time and are displaced the furthest with displacement decreasing gradually towards fault tip lines (Figure 16; Elliott, 1976). It is possible that in order to accommodate this differential movement within the thrust sheets of the Sawtooth Range, zones of mesoscale tear faulting (transport-parallel strike-slip faults) have developed, with left-lateral faults accommodating differential movement in the northern portions of the thrust sheet and right-lateral tear faults accommodating differential movement in the south (Figure 16). Alternatively, the development of localized zones of tear faulting may be related to local heterogeneities within the thrust sheet or variable tractions along the base of the thrust sheet.

Tear faults can occur throughout the BDZ and in general contribute the most fault length to the total fault intensity. These observations suggest that lateral variations in fault displacement or localized heterogeneities developed within or at the base of the thrust sheet during individual thrust events may be the most significant strain being accommodated by mesoscale mechanisms. The presence of tear faults appears to be the most significant factor controlling the pattern of minor fault intensities within the BDZs. In the Diversion and Beaver thrust sheets large peaks in total fault intensity are associated with peaks in tear faulting intensity suggesting that the transects through these thrust sheets included zones of concentrated tear faulting.

A)

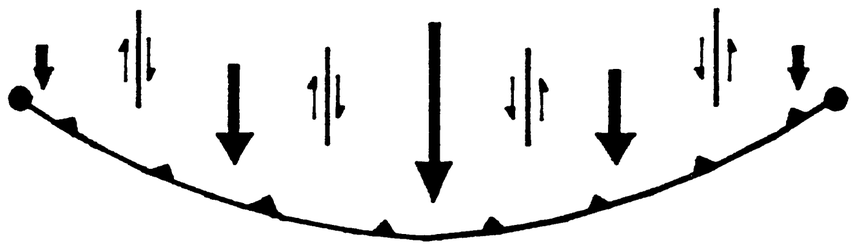

B)

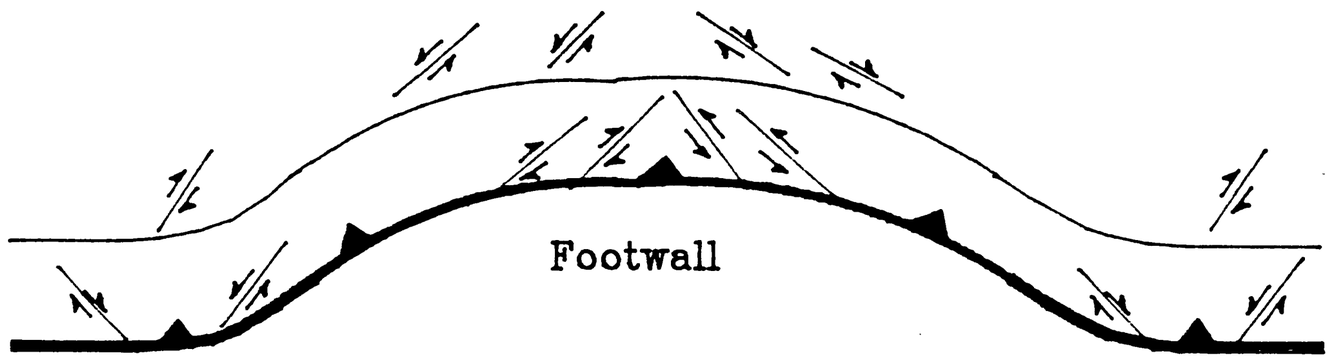

Figure 16 - A) Map view of the types of tear faults expected in a thrust sheet which has its maximum displacement at its center with displacement decreasing towards the tip lines. B) Strike parallel cross section view, showing the types and distribution of minor faults which might be expected as the hanging-wall accommodates movement over large scale asperities in the footwall.

The second type of strain being accommodated within the BDZ is range-parallel contraction and extension. Range-parallel extension is generally accommodated within the lower portion of a BDZ and may be separated from upper portions of the BDZ by a zone of strike parallel extension. These zones of strike parallel movement are possibly the result of movement of the hangingwall over asperities in the footwall (Figure 16). The decrease in the overall diversity of minor fault populations seen from the base of the thrust sheet to the upper portions of the BDZ is due in large part to the localization of strike parallel motion near the base of the BDZ indicating that the thrust sheet only accommodates those asperities relatively near the base.

Finally, the third type of strain found within the Sawtooth thrust sheets is manifested by the presence of synthetic and antithetic contraction faults and extension faults in the BDZs of the thrust sheets. These types of minor faults have been recognized previously (Wojtal, 1986; Woodward et. al., 1988). Wojtal (1986) attributed these fault types to heterogeneous simple shear within the thrust sheet. Zones of contraction and extension within the Sawtooth thrust sheets allow portions of the thrust sheet to be thickened or thinned and may be related to variable tractions along the thrust fault surface during motion (Platt and Leggett, 1986) or along bedding plane detachments within the thrust sheet. Contractional and extensional zones within the thrust sheet may

also be related to competency contrasts within the sheet.

The geometry of the minor fault populations within the Norwegian thrust sheet differs from the other Sawtooth thrusts studied. The relative unimportance of range-parallel convergence or divergence and the overall lower diversity of fault types may suggest a smoother fault surface at the base of the Norwegian thrust sheet. The dominance of tear faulting within the Norwegian thrust sheet suggests that the transect is located within a zone of localized across-strike movement.

Finite strain was found to be relatively constant within the thrust sheets independent of the intensity of the mesoscale deformation. This observation suggests that although mesoscale deformation occurs during thrust sheet emplacement grain scale deformation does not appear to be simply related to thrust motion. The strain values recorded in the thrust sheets are likely the result of a protracted strain history; perhaps including early bedding perpendicular compaction, thrust related strains, and late stage (post BDZ development) tectonic related compaction. The presence of a late tectonic compaction strain is indicated by the horizontality of the strain ellipsoids measured around a fold in the Teton River Valley. This late, post-thrusting, tectonic compaction may be the result of the truncation of the Sawtooth thrust sheets by out of sequence movement along the Lewis Thrust which is suggested to have overlain the Sawtooths. One high strain value and the presence of poorly developed cataclasites within the lowest 5%

of one BDZ suggests that limited intrablock deformation may have occurred during thrust faulting or possibly during fault propagation.

Conclusion

A balanced cross section indicates a minimum of 60% (10 km) shortening of the Paleozoic section across the central Sawtooth Range of the Montana Disturbed Belt. The shortening has been accommodated by a forward developing imbricate fan which was subsequently truncated by the Lewis Thrust.

Mesoscopic deformation within carbonates of the Sawtooth Range thrust sheets is accomplished by the development of mesoscale fault arrays which allow the base of the thrust sheet to deform by mesoscale cataclastic flow. Regional faults exhibit strain hardening behavior with the thickness of the BDZ increasing linearly as a function of increased thrust displacement. The relationship between thrust displacement and BDZ thickness suggests that displacement is approximately 33 times the BDZ thickness. BDZ thickness is independent of subsequent foreland deformation or fault shape.

At the base of a BDZ, there is a high diversity of minor fault types accommodating strike-parallel contraction and extension, lateral variations in thrust sheet displacement, and simple shear

within the thrust sheet. Only at the top of the BDZ do minor faults mimic the regional structure. At the top of the BDZ there is a much lower diversity of minor faults and they are dominantly dip or strike-slip accommodating simple shear and lateral variations in thrust sheet displacement. These various types of minor fault populations are commonly localized in thin deformational zones.

On a microscopic-scale, mechanical twinning, cataclasis, and pressure solution were the dominant deformation mechanisms indicating sub-greenschist deformation conditions. Finite strain determinations indicate a thin (<10m) zone of relatively high non-plane strain possibly related to intrablock deformation during cataclastic flow or fault propagation. In general, grain-scale deformation within the thrust sheet is relatively small and constant across the thrust sheet, and is independent of the intensity of the mesoscale deformation suggesting that in general mesoscale deformation and grain scale deformation are not coeval. The strain values likely also reflect a component of post BDZ, tectonic compaction related to the emplacement of the Lewis thrust sheet over the Mississippian carbonate thrust sheets of the Sawtooth Range to form a duplex by truncation of earlier underlying imbricates by a younger roof thrust.

References

Aleksandrowski, P., Graphical determination of principal stress direction populations: an attempt to modify Arthaud's method. Journal of Structural Geology, Vol.(7), (1985), pp. 73-82

Anastasio, D.J., Thrusting, halotectonics and sedimentation in the External Sierra, Southern Pyrenees, Spain., Unpublished Ph.D. Dissertation, Johns Hopkins University, Baltimore MD. (1987)

Anderson, E.M., The Dynamics of Faulting. Oliver and Boyd, Edinburgh, (1951), 206 pp.

Angelier, J., Determination of the mean principal direction of stresses for a given fault population. Tectonophysics, Vol. 56, (1979), pp. T17-T26.

Angelier, J., Tectonic analysis of fault slip data sets. Journal of Geophysical Research. Vol.(89), (1984), pp. 5835-5848.

Angelier, J., From orientation to magnitudes in paleostress determinations using fault slip data. Journal of Structural Geology. Vol.(11), (1989), pp. 37-50.

Arthaud, F., Methode de determination graphique des directions de raccourissement, d'allongement et intermediare d'une population de fauilles. Bulletin of the Geological Society of France, Vol (XI), (1969), pp. 729-732.

Bally, A.W., Gordy, P.L., and Stewart, G.A. Structure seismic data, and orogenic evolution of southern Canadian Rocky Mountains. Bulletin of Canadian Petroleum Geology, Vol. (14), (1966), pp. 337-381.

Bielenstein, H.U., The Rundle thrust sheet, Banff, Alberta. Ph.D. Dissertation, Queen's University, Kingston Ontario, (1969).

Clayton, J.L, Mudge, M.R., Lubeck, S.M., and Daws, T.A., Hydrocarbon source-rock evaluation of the Disturbed Belt, Northwestern Montana. Rocky Mountain Association of Geologists. Blake, R. editor. (1982), pp. 777-804.

Dunnet, D., A technique of finite strain analysis using elliptical particles. Tectonophysics, Vol (7), (1969), pp. 117-136.

Elliot, D., The energy balance and deformation mechanisms of thrust sheets. Philosophical Transactions of the Royal Society of London, series A, Vol. (283), (1976), pp. 289-312.

Erslev, E.A., Normalized center-to-center strain analysis of packed aggregates. Journal of Structural Geology, Vol. (10), (1988), pp. 201-209.

Erslev, E.A. and Ge, H., Least-squares center-to-center and mean object ellipse fabric analysis. Journal of Structural Geology, Vol. (12), (1990), pp. 1047-1059.

Etchcopar, A., Vasseur, G., and Daignieres, M., An inverse problem in microtectonics for the determination of stress tensors from fault striation analysis. Journal of Structural Geology, Vol (3), (1981), pp. 51-65.

Evans, J.P., Thickness-displacement relationships for fault zones. Journal of Structural Geology, Vol (12), (1990), pp. 1061-1065.

Fry, N., Random point distributions and strain measurment in rocks. Tectonophysics, Vol. (60), (1979), pp. 806-807.

Groshong, R.H., Low-temperature deformation mechanisms and their interpretation. Geological Society of America Bulletin., Vol. (100), (1988), pp. 1329-1360.

Hoeppener, R., Faltung and kluftung in nordteil des rheinischen scheifergebirges. Geol. Rundschau. Vol (41), (1953), pp. 144.

Hoffman, J., Hower, J., and Aronson, J.L., Radiometric dating of time of thrusting in the disturbed belt of Montana. Geology. Vol. (5), (1976), pp. 16-20.

Hull, J., Thickness-displacement relationships for deformation zones. Journal of Structural Geology. Vol (10), (1988), pp. 431-435.

Jaeger, J.C., The frictional properties of joints in rocks. Pure and Applied Geophysics. Vol. (43), (1959), pp. 148-158.

Klassen-Neklyodova, M.V., Mechanical twinning of crystals. New York, Consultants Bureau. (1964), 213 p.

Knipe, R.J., Deformation mechanisms - recognition from natural tectonites. Journal of Structural Geology. Vol.(11), (1989), pp. 127-146.

Lageson, D.R., Structural geology of the Sawtooth Range at Sun River Canyon, Montana Disturbed, Montana Geological Society of America Centenial Field Guide-Rocky Mountain Section. (1987), pp. 37-39.

Mitra, S., Duplex structures and imbricate thrust systems: geometry, structural position and hydrocarbon potential. American Association of Petroleum Geologists. Vol. (70), (1986), pp. 1087-1112.

Mudge, M. R., Bedrock geologic map of the Sawtooth Ridge quadrangle, Teton and Lewis and Clark counties, Montana: U.S. Geological Quadrangle Map. (GQ-381), (1965), scale 1:62,500.

_____, Geologic map of the Patricks Basin quadrangle, Teton and Lewis and Clark counties, Montana: U.S. Geological Survey Geologic quadrangle map. (GQ-453), (1966), scale 1:62,500.

_____, Structural geology of the Sun River Canyon and adjacent areas northwestern Montana: U.S. Geological Survey Professional Paper. (663-B), (1972), 52 p.

_____, Origin of the Disturbed Belt in northwestern Montana. Geological Society of America Bulletin. Vol. (81), (1970), pp. 377-392.

_____, A resume of the structural geology of the northern disturbed belt, Northwestern Montana. Rocky Mountain Association of Petroleum Geologists. (1982), pp. 91-122.

Mudge, M.R. and Earhart, R.L, Bedrock geologic map of part of the Northern Disturbed Belt, Lewis and Clark, Teton, Pondera, Glacier, Flathead, Cascade, and Powell Counties, Montana: U.S. Geological Survey Miscellaneous Investigation Series Map. (I-1375), (1983), scale1:125,000.

Norris, D.K., Structural conditions in Canadian coal mines. Bulletin of the Geological Survey of Canada. Vol. (44), (1958), pp. 1-54.

Otsuki, K., On the relationship between the width of shear zone and the displacment along fault. Journal of the Geological Society of Japan. Vol.(84), (1978), pp. 661-669.

Platt, J.P., and Legget, J.K., Stratal extension in thrust footwalls, Makran accretionary prism: implications for thrust tectonics. American Association of Petroleum Geologists. Vol. (70), (1986), pp. 191-203.

Price, R.A., The tectonic significance of mesoscopic subfabrics in the southern Rocky Mountains of Alberta and British Columbia. Canadian Journal of Earth Sciences. Vol. (4), (1967), pp. 39-70.

Reches, Z., Analysis of faulting in a three-dimensional strain field. Tectonophysics. Vol (47), (1978), pp. 109-129.

Reches, Z., Determination of the tectonic stress tensor from slip along faults that obey the Coulomb yield condition. Tectonics. Vol (6), (1987), pp. 849-861.

Robertson, E.G., Relationship of fault displacement to gouge and breccia thickness. Mining Engineering. Vol. (35), (1983), pp. 1426-1432.

Stearns, D.W., Fracture as a mechanism of flow in naturally deformed layered rocks. Geological Survey of Canada. Special Paper, 68-52, (1969), pp. 79-95).

Wojtal, S., Deformation within foreland thrust sheets by populations of minor faults. Journal of Structural Geology. Vol.(8), (1986), pp. 341-360.

Wojtal, S., and Mitra, G., Strain hardening and strain softening in fault zones from foreland thrusts. Geological Society of America Bulletin. Vol. (97), (1986), pp. 674-687.

Woodward, N.B., Wojtal, S., Paul, J.B., and Zadins, Z.Z., Partitioning of deformation within several external thrust zones of the Appalachian Orogen. Journal of Geology. Vol.(96), (1988), pp. 351-361.

Appendix 1

A Fieldtrip Guide to the Structural geology of the Sawtooth Range, Montana

Introduction

The Sawtooth Range is one of the best exposed examples of a fold thrust belt in the western United States. It is an outstanding classroom for the demonstration of the processes involved in foreland fold and thrust belt development. The exposures available along the Sun River Canyon provide an excellent opportunity to observe the manner in which foreland carbonate thrust sheets deform during emplacement. This field guide is intended to show the regional scale geometry of the Sawtooth Range structures as well as the character of mesocale features developed within the Sawtooth thrust sheets.

Roadside stops

The following localities are on the road (Montana 435, U.S. Forest Service Road 208) between Augusta, Montana, and the trail head at Gibson Dam in the Sun River Canyon (figure 18). The total mileage of the traverse is 26 miles and all mileages are given from the intersection of U.S. 287 and Montana 434-435 in Augusta.

Stop 1 is located at Gibson Overlook (24.1 miles). Gibson Overlook is located in the hanging wall of the Beaver Thrust sheet at the crest of a ridge formed by the resistant Mississippian Castle

Reef Dolomite. The panoramic view to the east shows the thrust sheets of the lower Sun River Canyon which include the Diversion, Home, French, and Norwegian thrust sheets. To the south, the Beaver and Norwegian thrust sheets form spectacular dip slopes on the Mississippian Castle Reef Dolomite.

Stop 2 is located .3 miles east from stop 1 (23.7 from Augusta). The Beaver thrust is exposed within the steep hillside to left, where the Mississippian Allan Mountain Limestone has been thrust over the Cretaceous Colorado Group (Mudge, 1972). Within the hanging wall of the Beaver thrust sheet deformation has been partitioned into mesoscale fault arrays which may in some cases is localized into "shattered zones" (see main text for explanation and photograph of shattered zones), these minor faults and shattered zones are exposed along this roadcut.

Stop 3 is located .7 miles east of stop 2 (23 miles from Augusta) at the north side of the bridge across the Sun River. The stop is located in a river exposure of the Castle Reef Dolomite on the west bank of river just south of the bridge. This bed displays the different mechanical behavior of dolomite and limestone within the Sawtooth thrust sheets. The highly fractured beds are dolomite. The interlayered limestone beds have deformed more continuously than the dolomites.

Stop 4 is located 1.2 miles from stop 3 (21.8 miles from Augusta). The roadside exposure on the south side of the road provides an excellent exposure of the French thrust fault which places the Missippian Allan Mountain Limestone on shales of the Cretaceous Colorado Group. As in the Beaver thrust sheet,

deformation has been partitioned in an interlocking network of minor faults which have allowed the base of the thrust sheet to deform (see figure 5 in the main text).

Stop 5 is 4.8 miles from stop 4 (17 miles from Augusta). South of the road is a well-exposed, overturned, thrust-faulted anticline in the Cretaceous Colorado Group. The forelimb and backlimbs of this asymmetric anticline have both been thrust faulted. This is an excellent example of the style of deformation found within the Cretaceous rocks of the foothills of the thrust belt. (Lageson, 1987)

Stop 6 (optional) is located 26 miles from Augusta and is at the end of the road. This is the boat access for Gibson Reservoir and the trail head for U.S. Forest service trail 201. A short hike along this trail offers good exposures of Devonian and Cambrian strata along the Palmer thrust fault (figure 18) (Lageson, 1987).

Stop 7 (optional) is located approximately 21 miles from Augusta along the Pishkun irrigation canal. Cretaceous rocks exposed within this canal are imbricated by many closely spaced imbricate faults with relatively small offsets, a style of deformation characteristic of Subbelt1.

For additional information please see the following references.

Lageson, D.R., 1987, Structural geology of the Sawtooth Range at Sun River Canyon, Montan Disturbed Belt, Montana, in The Geological Society of America Centenial Field Guide-Rocky Mountain Section, pp. 37-39.

Mudge, M. R., 1965, Bedrock geologic map of the Sawtooth Ridge quadrangle, Teton and Lewis and Clark counties, Montana: U.S. Geological Quadrangle Map, GQ-381, scale 1:62,500.

_____, 1966, Geologic map of the Patricks Basin quadrangle, Teton and Lewis and Clark counties, Montana: U.S. Geological Survey Geologic quadrangle map, GQ-453, scale 1:62,500.

_____, 1972, Structural geology of the Sun River Canyon and adjacent areas northwestern Montana: U.S. Geological Survey Professional Paper 663-B, 52 p.

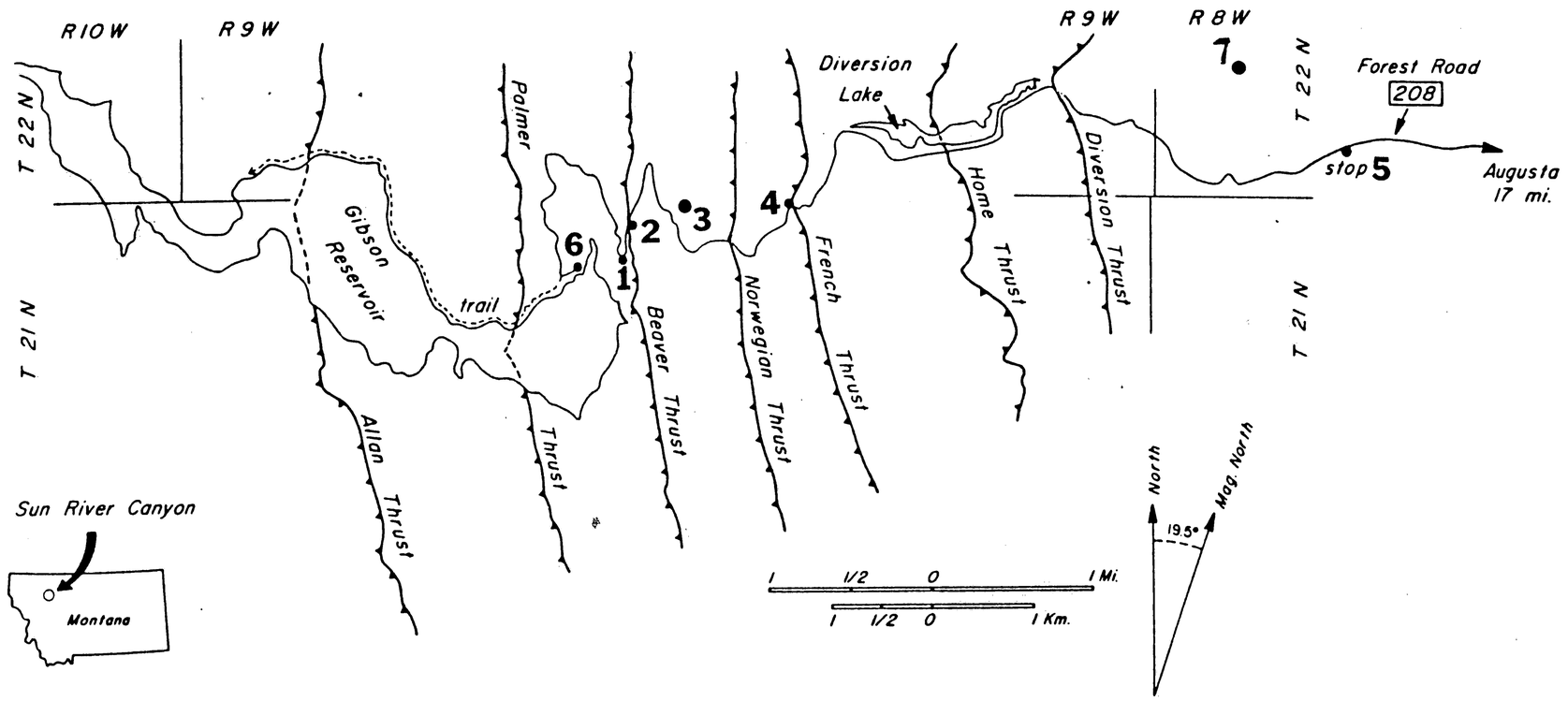

Figure 17 - Map of the lower Sun River Canyon showing stop localities along Forest Service Road 208, major thrust faults, and Gibson Reservoir and Diversion Lake (from Lageson, 1987).

Appendix 2

Future Work

Previous study documents the presence of a considerable amount of along strike and oblique movement within the BDZs of foreland thrust sheets. This movement is difficult to constrain with only one cross section. Possible future work would involve an additional minor fault traverse within the thrust sheets located along Deep Creek. Deep Creek is located to the north of the Sun River Canyon and cross cuts the same portion of the Sawtooth Range as previous traverses completed along the Sun River. This additional traverse would provide important insight into the three dimensional characteristics of minor fault deformational zones within a thrust sheet by allowing along strike variations in BDZ characteristics to be determined. In addition measurement of thrust sheet displacement and the thickness of the BDZs will provide additional data towards establishing a relationship between BDZ thickness and displacement within foreland carbonate thrust sheets. Data gathered along a Deep Creek traverse will also provide a more complete picture of across strike variations in BDZ thickness. It may also be possible to collect finite strain data within the lowest 10 m of these thrust sheets thereby providing additional insight into the state of finite strain at the base of a thrust sheet.

Deformation at the base of thrust sheets has been likened to cataclastic flow (Stearns, 1969) as minor faults developed within

the BDZ form an interlocking network which surround supposed rigid blocks of material. This minor fault network allows the base of the thrust sheet to deform by the rotation of the fault-bound blocks relative to each other. In order to test this model of thrust sheet deformation future work could involve an analysis of finite strain across individual fault bound blocks to determine the distribution of strain within these blocks. The high quality of exposure and the previous recognition of an interlocking network of faults make the base of the French thrust sheet the most logical place in which to complete this work.

Appendix 3

Vita

James Edward Holl

Department of Geological Sciences
Lehigh University
#31 Williams Hall
Bethlehem, Pa. 18015-3188
215/758-3702

234 E. Susquehanna St.
Allentown, Pa., 18013
215/797-3220

PERSONAL:

Born 20 August 1965
Erie, Pa.

CURRENT POSITION: (1989-)

Ph.D. student, Department of Geological Sciences, Lehigh University, Bethlehem, Pa., Thesis Advisor, David J. Anastasio

EDUCATION:

M.S. Lehigh University. Structural Geology, January 1990. "Deformation Mechanisms and Finite Strain within the Foreland Imbricate Fan, Sawtooth Range, Montana", Thesis Advisor, David J. Anastasio

B.S. Allegheny College. Geology Major, 1987. "Progressive Development of Strain-Related Features in Anorthositic Rocks from the Grenville Province of the Canadian Shield", Thesis Advisor, Wayne Brewer

PROFESSIONAL EXPERIENCE:

- Research Assistant, NSF Grant EAR 8816335, "Thrusting and Halotectonics in the Spanish Pyrenees", Department of Geological Sciences, Lehigh University, Bethlehem, Pa. (1989-1990).

- Assistant Geologic Consultant, Newburg, Walker, Rogers, Pennsylvania Turnpike Lehigh Tunnel Project, (October, 1990).
- Five years of field experience in the Appalachians, United States Rockies, Canadian Shield, and the Pyrenees (1986-1990).
- Analytical experience with a CTF 2-axis cryogenic magnetometer, a Molspin spinner magnetometer, a Schonstedt GSD-5 tumbling alternating field demagnetizer, and a Schonstedt TSD-1 thermal demagnetizer (1989-1990).
- Teaching Assistant, Department of Geological Sciences, Lehigh University, Bethlehem, Pa. (1987-1989), courses taught include Structural Geology, Geophysics, Physical Geology, Environmental Geology, Historical Geology, Gemology, and Geology for Engineers.
- Laboratory Technician for X-ray Diffractometer, Lehigh University, Bethlehem, Pa. (June and July 1989).

PROFESSIONAL ACTIVITIES AND AFFILIATIONS:

Member:

Geological Society of America
American Association of Petroleum Geologists
Sigma Xi

Fellowships:

1990-1991 Lehigh University ($18,680)

Grants:

1990 "Rates and Geometries of Thrusting and Salt Deformationin the Spanish Pyrenees"
- Geological Society of America ($850)
- American Association of Petroleum Geologists ($650)
- Sigma Xi ($400)

1989 "Rates and Geometries of Thrusting and Salt

Deformation in the Spanish Pyrenees"
- Geology Department Research Fund ($1000)

1988 "Deformation and Finite Strain within the Foreland Imbricate Fan, Sawtooth Range, Montana"
- American Association of Petroleum Geologists ($800)
- Sigma Xi ($400)
- Standard Oil of California Research Grant ($600)

Publications:

1990 Transverse Fold Development in the South Pyrenean Thrust Belt, Spain. Geological Society of America, Abstracts with Programs, 22:(7), p. A225 (with D. Anastasio).

1989 Deformation Mechanisms and Finite Strain within the Foreland Imbricate Fan, Sawtooth Range, Montana. Geological Society of America, Abstracts with Programs, 21:(6), p. A224 (with D. Anastasio).

1988 The Role of Microscopic and Macroscopic Deformation Mechanisms in Progressively Deformed Anorthositic Rocks from the Parry Sound Shear Zone, Ontario, Canada. Geological Society of America, Abstracts with Programs, 20:(1), p. 27.

in prep: Deformation Mechanisms and Finite Strain within the Foreland Imbricate Fan, Sawtooth Range, Montana. To be submitted to the Bulletin of the Geological Society of America (with D. Anastasio).

in prep: Transverse Fold Development in the South Pyrenean Thrust Belt, Spain. To be submitted to Geology (with D. Anastasio).